# Cookoff Results of Sub-scale Hazard Division 1.3 Propellant Samples

Eric Wilson, Matthew Gross, Ephraim Washburn,
Eric Sievert, Daniel Wooldridge, John Daly
*Naval Air Warfare Center Weapons Division, China Lake, California*

Scott Barry
*Jacobs Technology Naval Systems, Ridgecrest, California*

J. Covino
*Policy Development Division*
*Department of Defense Explosives Safety Board, Alexandria, Virginia*

## INTRODUCTION

A hazardous materials siting effort by the National Aeronautics and Space Administration (NASA), the Naval Air Warfare Center Weapons Division (NAWCWD), Hughes & Associates, Inc., and Alliant Techsystems Inc. (ATK), indicated that inadvertent ignition of a rocket in the Vehicle Assembly Building (VAB) at Kennedy Space Center (KSC) might cause other rockets in the facility to burn. Currently, the Space Shuttle Program (SSP) builds and stores rockets in the VAB. The Constellation Program, which was to replace the Shuttle, would have assembled and stored a much greater amount of Hazard Division 1.3 material in the VAB. In order to accurately determine the hazard to the VAB due to this new amount of material, an analysis and modeling study was conducted. Two scenarios were considered. The first was ignition of other rockets due to hot combustion products entering the bore of the other motors. The second was the ignition of other rockets from heat flux penetrating through the motor case. Of these two, the most likely scenario was deemed to be ignition through the motor bore. However, no data existed for time to ignition through the case of a large rocket motor at flux levels representative of a cookoff situation. Ignition was modeled for both scenarios. In the through-the-case model, the heat flux that would be applied to the case of a motor was estimated to be 300 $kW/m^2$. Further modeling indicated that the time to ignition through the case of the motor would be approximately 4 minutes.

Figure 1 shows the flux/time region of interest to the NASA-led effort. No data from production samples was available in the low flux/long time region of the graph. Previously, data were generated using bare propellant to investigate operational ignition scenarios (high flux/short times). The NAWCWD test series provided data on time to ignition of a production sample, through the case, at low flux. Comparing these new “cased” data to the previous “uncased” data is accomplished by considering the total energy input into the sample, rather than the power (flux) of the heat source. Some concerns regarding the location (trend) of the new data as well as the suitability of the model used to generate them are addressed, but the method shows promise as a predictive tool for ignition of Hazard Division 1.3 production samples, both cased and uncased, with implications for cookoff prediction capability for actual rocket motors, as well.

# Report Documentation Page

*Form Approved*
*OMB No. 0704-0188*



| | | |
|---|---|---|
| 1. REPORT DATE<br>**JUL 2010** | 2. REPORT TYPE<br>**N/A** | 3. DATES COVERED<br>**-** |
| 4. TITLE AND SUBTITLE<br>**Cookoff Results of Sub-scale Hazard Division 1.3 Propellant Samples** | | 5a. CONTRACT NUMBER |
| | | 5b. GRANT NUMBER |
| | | 5c. PROGRAM ELEMENT NUMBER |
| 6. AUTHOR(S) | | 5d. PROJECT NUMBER |
| | | 5e. TASK NUMBER |
| | | 5f. WORK UNIT NUMBER |
| 7. PERFORMING ORGANIZATION NAME(S) AND ADDRESS(ES)<br>**Naval Air Warfare Center Weapons Division, China Lake, California** | | 8. PERFORMING ORGANIZATION REPORT NUMBER |
| 9. SPONSORING/MONITORING AGENCY NAME(S) AND ADDRESS(ES) | | 10. SPONSOR/MONITOR'S ACRONYM(S) |
| | | 11. SPONSOR/MONITOR'S REPORT NUMBER(S) |

12. DISTRIBUTION/AVAILABILITY STATEMENT
**Approved for public release, distribution unlimited**

13. SUPPLEMENTARY NOTES
**See also ADM002313. Department of Defense Explosives Safety Board Seminar (34th) held in Portland, Oregon on 13-15 July 2010, The original document contains color images.**

14. ABSTRACT

15. SUBJECT TERMS

| 16. SECURITY CLASSIFICATION OF: | | | 17. LIMITATION OF ABSTRACT | 18. NUMBER OF PAGES | 19a. NAME OF RESPONSIBLE PERSON |
|---|---|---|---|---|---|
| a. REPORT<br>**unclassified** | b. ABSTRACT<br>**unclassified** | c. THIS PAGE<br>**unclassified** | **SAR** | **45** | |

**Standard Form 298 (Rev. 8-98)**
Prescribed by ANSI Std Z39-18

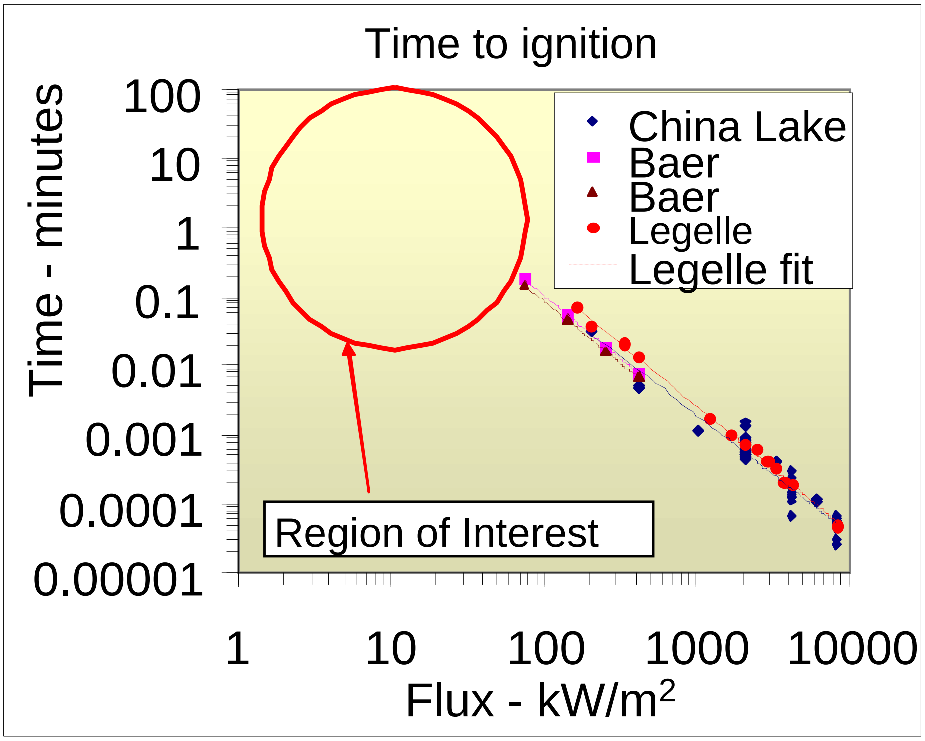


Figure 1. Flux-Time Region of Interest for Cookoff. No data existed for this region.

**METHOD**

Samples were obtained from the propellant manufacturer. Twenty samples were prepared. The samples were arranged to simulate the outer layers of the system under study. The samples incorporated a steel case, an insulator, a liner, and propellant. These samples were heated by a propane/oxygen torch, one at a time. The time elapsed from the start of flame impingement to propellant ignition was determined from a video recording of the test event. The incident heat flux provided by the impinging flame was measured using a Gardon gauge heat flux sensor.

The samples designed to simulate the outer layers of the rocket motor under study were contained in a 6-inch length of 4-inch diameter schedule-10 welded pipe. Three threaded holes in one end of each pipe section allowed set-screws to hold the steel case simulator in place. In order to minimize thermal conduction from the pipe to the sample inside, a layer of fiberglass insulation was attached to the inside of the pipe. The insulation thickness was 0.125 inch and was intended to insulate the propellant from the pipe wall during testing. Figures 2 through 6 illustrate how the samples were constructed. Figure 2 shows the layers of the samples from bottom to top. At the bottom, a piece of 0.5-inch-thick steel was used to simulate the motor case. This steel was primed and painted white on the outside. Insulation was attached to the other side (inside) of the steel using a bonding agent. Liner material was then cast on top of the insulation and propellant was cast on top of the liner.

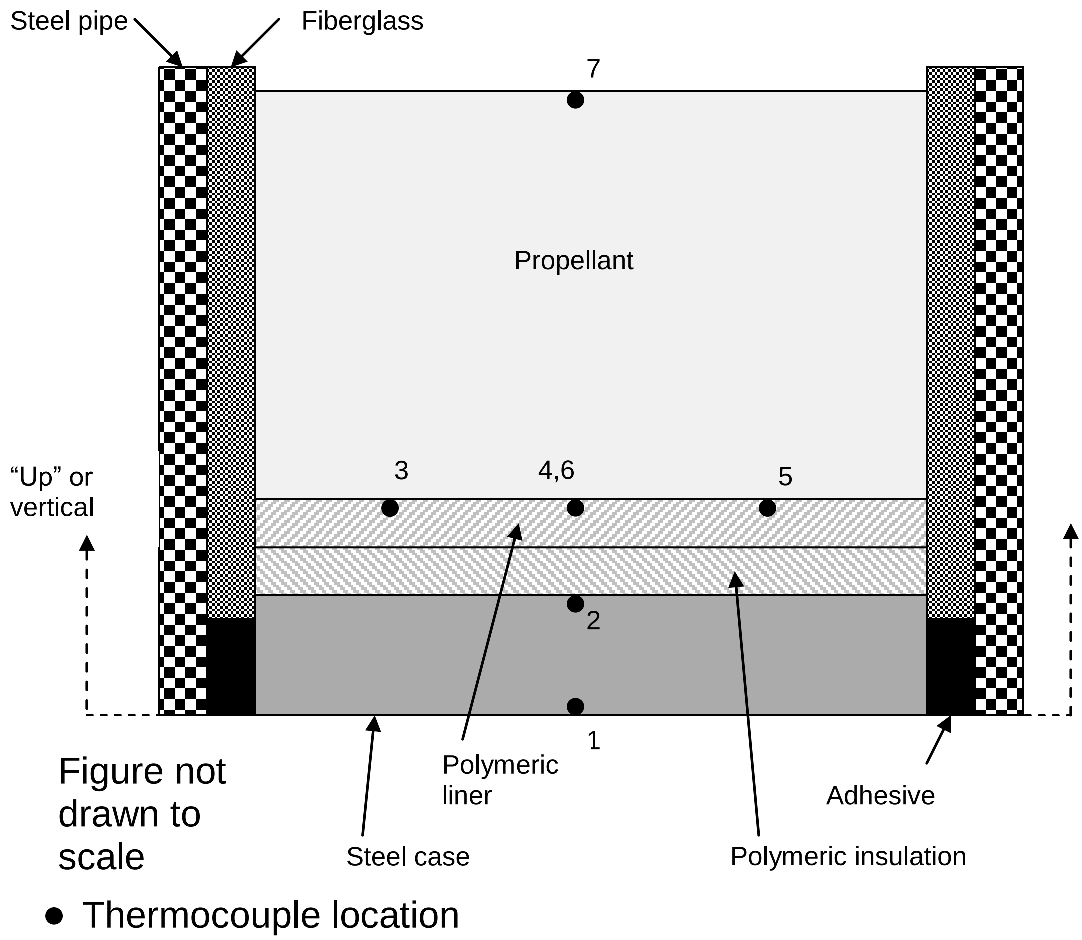


FIGURE 2. Notional Drawing of Sample Showing Thermocouple Locations (Side View).

The case simulator was fabricated from D6AC steel. Screw-set notches were machined in the edge of the steel to accommodate pins to hold the steel in place in one end of the pipe. In order to minimize thermal conduction from the case to the pipe, alumina bolts were used as the set-screw pins. Additionally, the annulus between the inner wall of the pipe and the outer edge of the steel case was filled with an adhesive in order to block entry of flame and hot gas from the heat source behind or past the outer (front) face of the steel. Heating of the sample was intended to occur through the steel case, and efforts such as filling the annulus were made to avoid heating from the sides of the sample. The outer surface of the steel case was painted with zinc-rich epoxy-polyamide primer and epoxy-polyamide top coat (white) paint.

The insulator used was 100-mil-thick nitrile-butyl rubber (NBR). The back surface of the steel case was prepared with primer and bonding agent in order to attach the insulation to the steel. The liner was a 65-mil-thick polymer that required curing to solidify. In order to place the thermocouples precisely at the liner/propellant interface, a method was envisioned that would partially cure the liner so that its surface was tacky and would hold the thermocouple bead on the liner surface until propellant was cast on top of it. However, this effort was not successful, and epoxy was used to hold the beads in place during propellant casting.

The propellant was vacuum-cast into the pipe/fiberglass/case/insulator/liner assembly to a depth of 3 inches. This thickness of propellant has been found to offer sufficient thickness that modeling boundary conditions can assume an infinite thickness. The propellant under test was polybutadiene acrylonitrile copolymer (PBAN) with ammonium perchlorate (AP) and aluminum powder composite solid grain with approximately 80 percent solids loading.

Although this test series was primarily interested in time to ignition, thermocouples were placed at certain locations in an attempt to investigate the response of the system as it was heated. Type-K thermocouples were used; one was welded to the outer face of the case simulator, at the center. This was later painted over along with the outer face itself. Another thermocouple was placed between the steel case and the insulation. Four thermocouples were located at the interface of the liner material and the propellant. These four 'interface' thermocouples were attached to the liner using a small amount of epoxy. The rear-most thermocouple was located on the back surface of the propellant, at the center. This last thermocouple was installed just prior to testing.

The four thermocouples located at the liner/propellant interface were placed 1 inch from the centerline at 90 degree intervals. Figure 2 shows the arrangement as viewed from the side of the sample. Figure 3 shows the arrangement as viewed from the top.

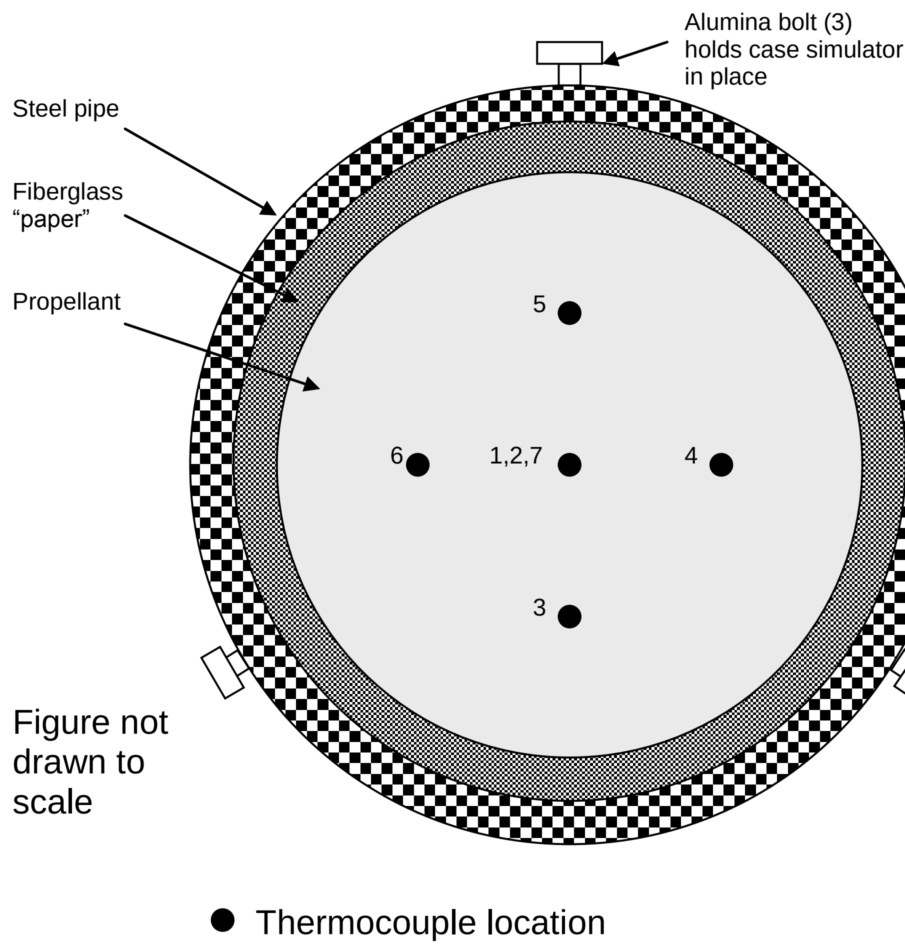


FIGURE 3. Notional Drawing of Sample Showing Thermocouple Locations (Top View).

Several photographs show the finished sample condition prior to installation in the test device. Figure 4 shows the D6AC steel surface that was painted white where the heat flux was applied. Figure 5 shows a side view of the sample. Figure 6 shows the top-most surface of the propellant inside the back section of the sample-holder pipe and the fiberglass layer.

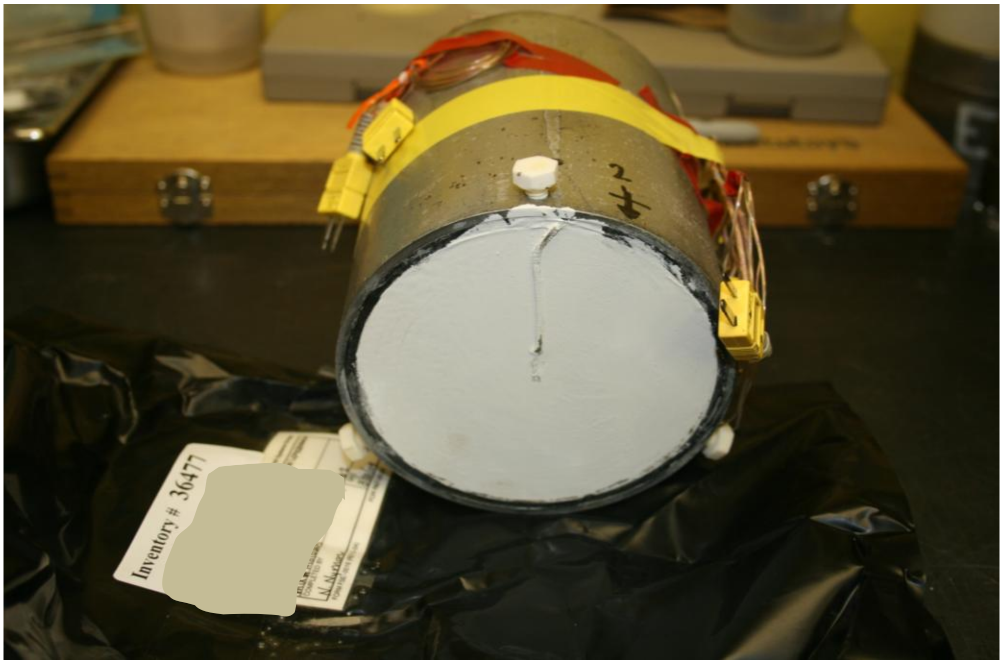


FIGURE 4. Sample Outermost Case Painted White (Heat Flux Applied to this Painted Surface).

FIGURE 5. Sample Side View.

FIGURE 6. View of Top-Most Surface of Propellant in Sample Holder Pipe and Fiberglass Layer.

Samples were heated using a propane/oxygen torch and test device developed at NAWCWD. The torch was designed with 89 coaxial fuel and oxygen feeds supplied by compressed gas cylinders. The resulting flamelets were approximately 6 inches in length, with an overall flame height of approximately 18 inches. Since the flamelet from each fuel/oxygen coaxial feed was located near its neighbors, a relatively flat flame surface was created at the tips of the flamelets. Figure 7 shows the flame from the torch. The heat flux from this torch was investigated and maximized. Then, heat flux at the sample face was varied by moving the torch toward or away from the sample face.

The torch was installed in a test device that functioned to hold the sample and the torch in place. It consisted primarily of an insulated steel plate with a hole in the middle of it where the sample was placed. As seen in Figure 8, the diameter of the hole in the test device plate was smaller than the diameter of the sample's steel case; this was designed to limit any flame impinging either the adhesive in the pipe/case annulus or the outer pipe. The torch rested directly below the hole at a distance selected to achieve the desired heat flux. The torch/sample holder assembly was designed to deliver heat fluxes between 50 $kW/m^2$ and 300$kW/m^2$, depending on the distance of the torch from the sample.

Water-cooled heat-flux transducers (Medtherm 64-50-20 Gardon Gauge) were used to determine the amount of heat flux reaching the sample face. These sensors have a maximum designed flux limit of 500 $kW/m^2$. One gauge was installed in the sample holder plate next to the sample hole, facing the incoming flame. The other gauge was mounted in a pipe/disk arrangement similar to the sample assembly construction. This assembly was located on the test device, just as samples were located. In this manner, both gauges faced the flame, one from the sample location, and one located 4.5 inches to one side of the center of the sample location. Figure 7 shows the arrangement of both gauges in the test device. The sample-location gauge was removed and replaced with a sample during testing, but the other gauge remained installed to measure the heat flux during tests. Good agreement between the two gauges during calibration of the torch indicated that the real-time test heat flux measurements from the gauge to one side of the sample provided a very good indication of the heat flux that impinged the sample.


FIGURE 7. Test Device Flame Impingement Area Showing Both Heat Flux Gauges Mounted in the Device.

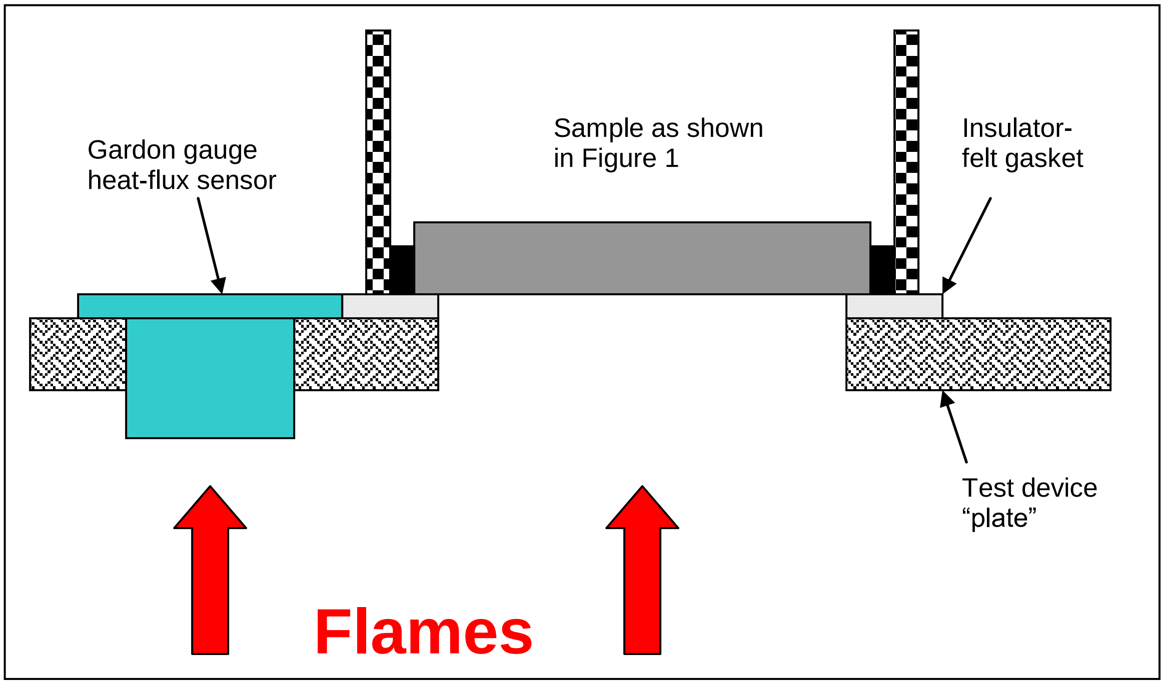


FIGURE 8. Drawing of Sample Size Versus Test Device Hole (With Felt Gasket)
and Showing Heat Flux Sensor Location.

Data were acquired using a National Instruments cDAQ 9172 system containing three National Instruments 9211 low-voltage signal conditioning modules. Data signals were conditioned and then sent to a laptop computer running National Instruments Signal Express software, which acquired and recorded the data. Data were collected at 2 Hz. Also, video was captured during testing. Data reduction was accomplished using National Instruments DIAdem software package.

Samples were thermally conditioned to 21°C (70°F) prior to testing. Test setup was accomplished by connecting the thermocouples to the data acquisition system and setting the sample on the test device above the torch. A piece of insulator felt (Lamination Technologies LT cloth) was placed between the outer pipe of the sample holder and the test device plate to minimize thermal conduction. In addition, it served to block flames reaching the outside of the sample pipe due to any misalignment of the sample (see Figure 7). Once the sample was in place, a layer of insulator felt was wrapped around the sample and secured to avoid hot gas impingement on the outside or back of the sample.

Samples were heated with the burner for up to 10.5 minutes for the first test series (June 2009) or up to 38.2 minutes for the second test series (April 2010) or until propellant ignition occurred. The heat flux applied to the samples was varied by changing the distance between the torch to the sample. Three heat flux levels were chosen as goals for heating: 300, 200, and 100 kW/$m^2$. Samples were tested at each flux level and the Gardon gauge transducer recorded the flux applied to each sample. Actual flux varied during each test and from test to test, as shown by the flux data. Average flux applied in each test is reported. During heating, the video feed was monitored for sample ignition. When ignition was detected, the torch was secured.

## RESULTS

A summary of the results are presented in Table 1. Figure 9 presents a graph of heat flux versus time to ignition.

TABLE 1. Time to Propellant Ignition at Certain Average Heat Fluxes.

| Sample number | Average Heat Flux, kW/m$^2$ | Time, sec |
|---|---|---|
| 16 | 296 | 220.5 |
| 19 | 289 | 210.5 |
| 9 | 295 | 181.5 |
| 4 | 225 | 275.5 |
| 14 | 215 | 280 |
| 20 | 177 | 286 |
| 13 | 65 | 633 – did not ignite |
| 6 | 72 | 636 – did not ignite |
| 18 | 55 | 633 – did not ignite |
| 10 | 277 | 241 |
| 1 | 260 | 213 |
| 2 | 231 | 301 |
| 5 | 156 | 412 |
| 11 | 157 | 969 |
| 8 | 149 | 882 |
| 12 | 63 | 2,292 |
| 15 | 37 | 1,698 – did not ignite |
| 17 | 84 | 1,065 |
| 3 | 63 | 1,301 |
| 7 | 60 | 1,007 |

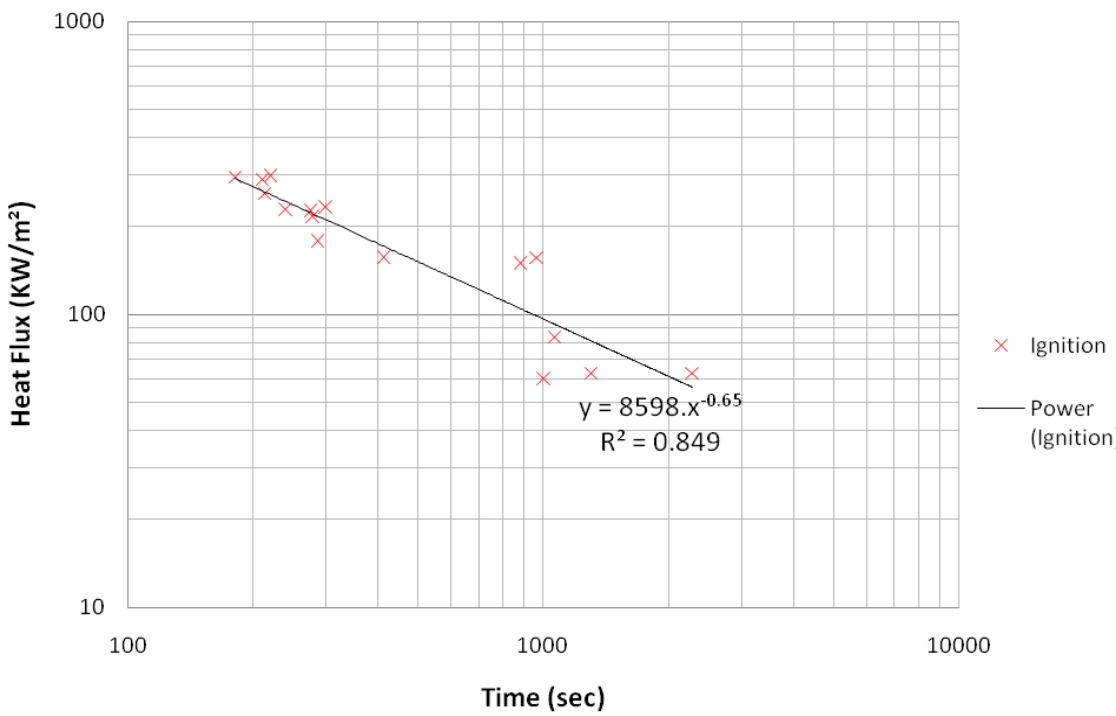


FIGURE 9. Time to Ignition Versus Heat Flux for Production Samples Heated Through the Case. Data do not include samples 6, 13, 15, 18.

Summary data sheets in Figures 10 through 29 show the applied flux, thermocouples response, and time to ignition (or time of burn) for each test. Certain other values are also presented, such as the average heat flux and the heat flux variability during the test. No heating was evident through to the back of the 3-inch thickness of propellant during testing as measured by thermocouple at the back surface of the propellant grain (except when allowed to heat-soak for long periods of time during the extended burn of samples that did not ignite).

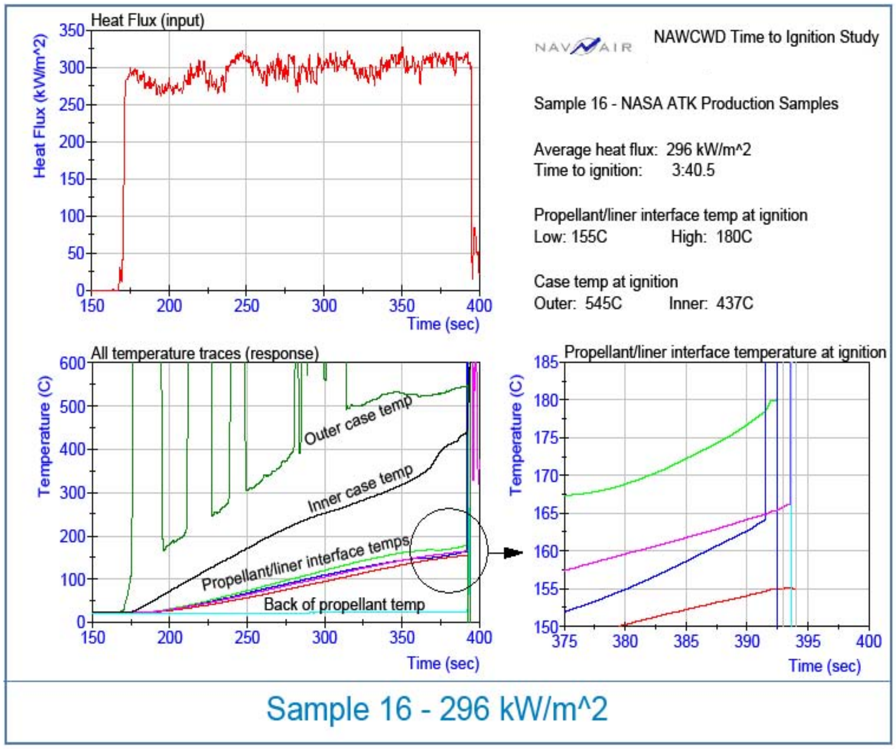


Notes: Outer (front-most) thermocouple intermittent
Flux variability during burn – 262 to 326 kW/m$^2$

FIGURE 10. Sample 16 Data.

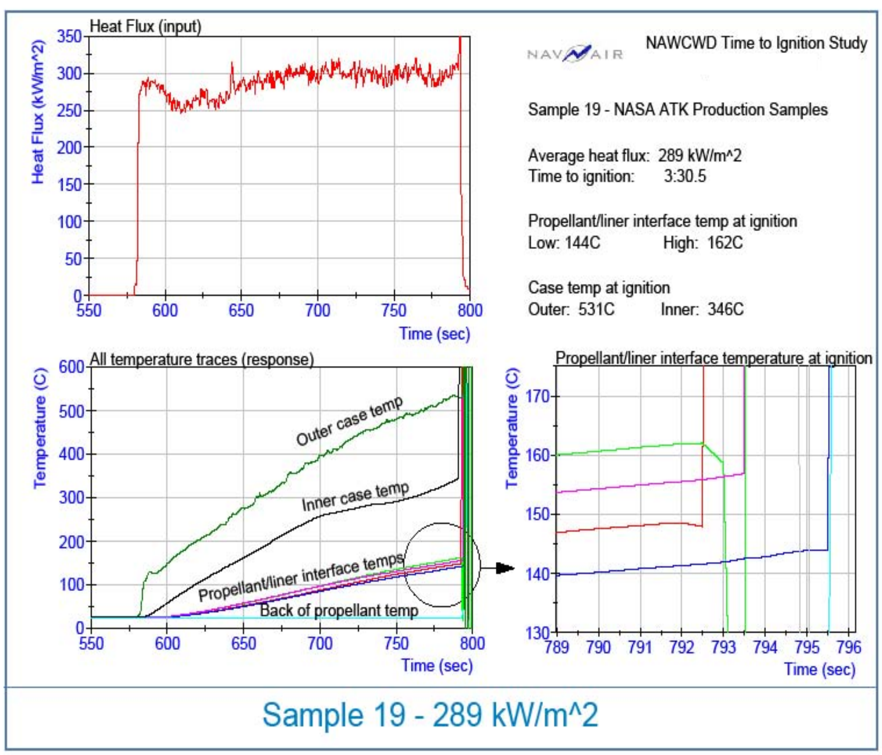


Notes: Flux variability during burn: 246 to 321 kW/m$^2$

FIGURE 11. Sample 19 Data.

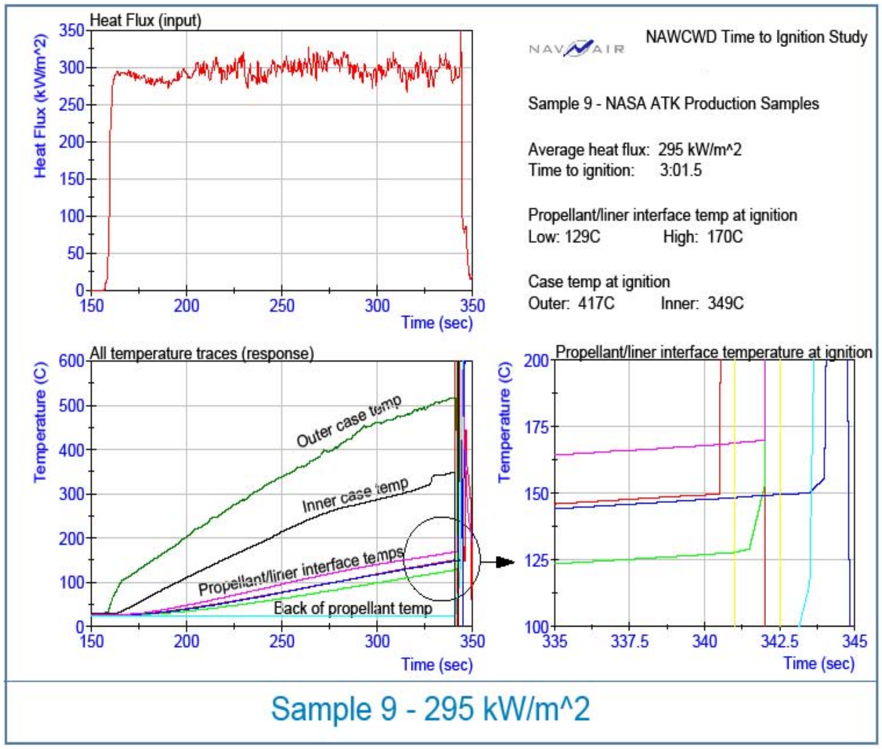


Notes: Flux variability during burn: 267 to 327 kW/m$^2$

FIGURE 12. Sample 9 Data.

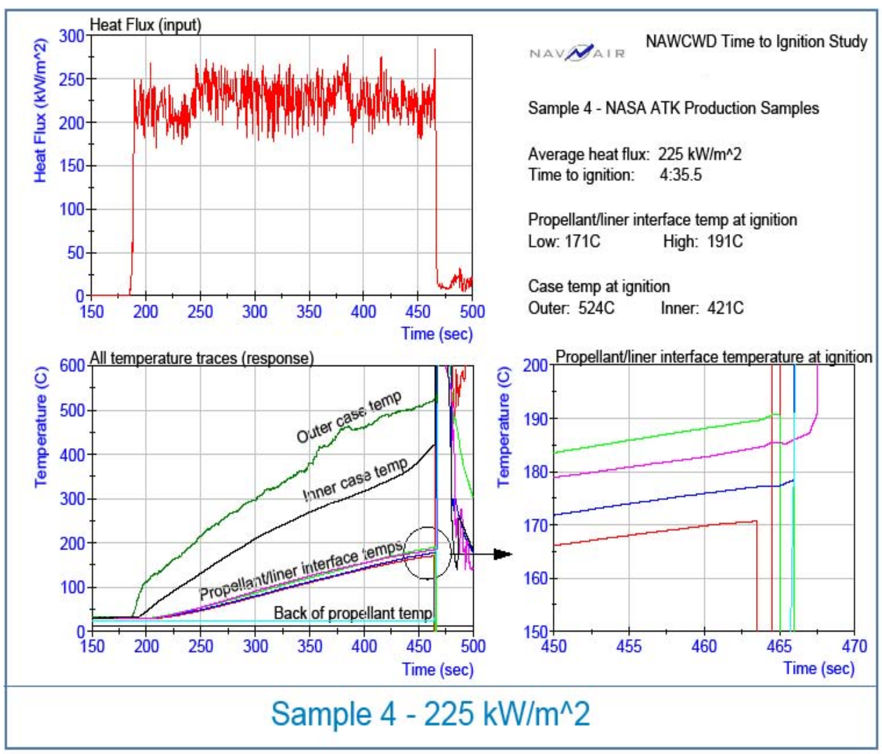


Notes: Flux variability during burn: 171 to 276 kW/m$^2$

FIGURE 13. Sample 4 Data.

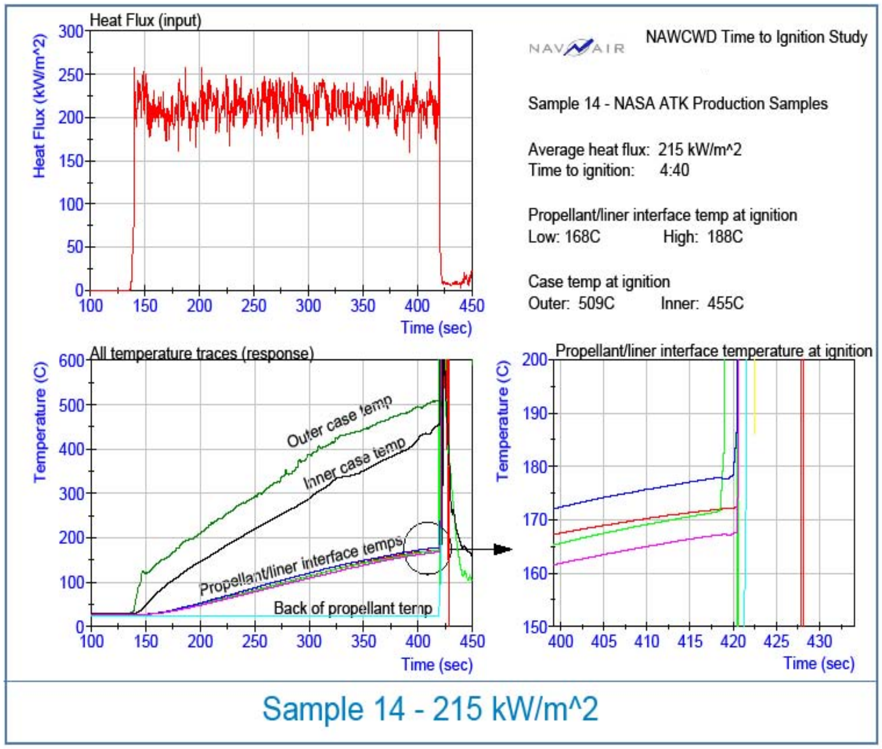


Notes: Flux variability during burn: 161 to 257 kW/m$^2$

FIGURE 14. Sample 14 Data.

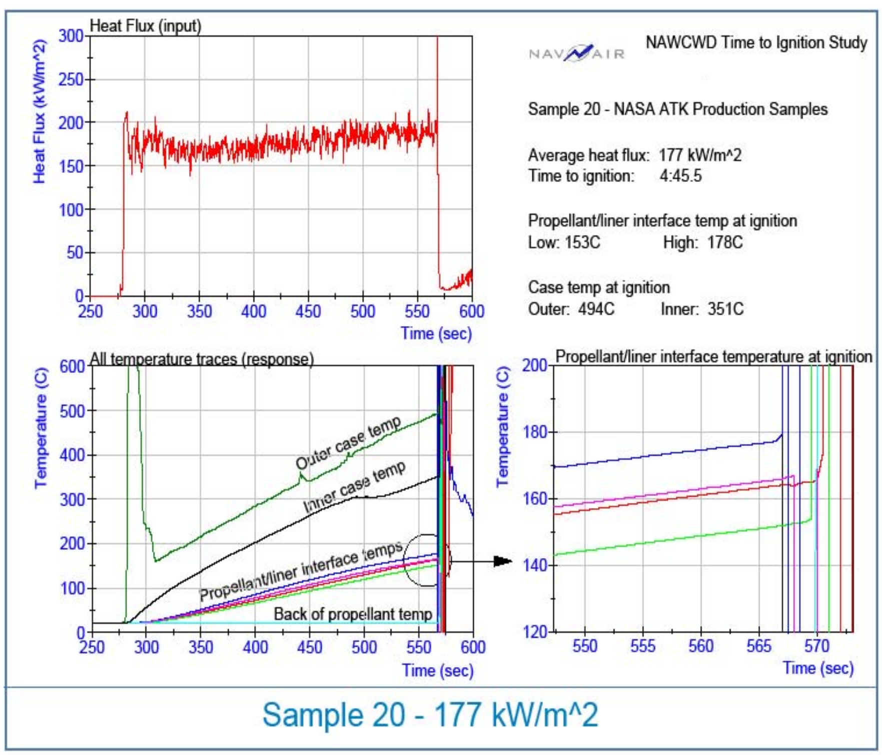


Notes: Flux variability during burn: 139 to 215 kW/m$^2$

FIGURE 15. Sample 20 Data.

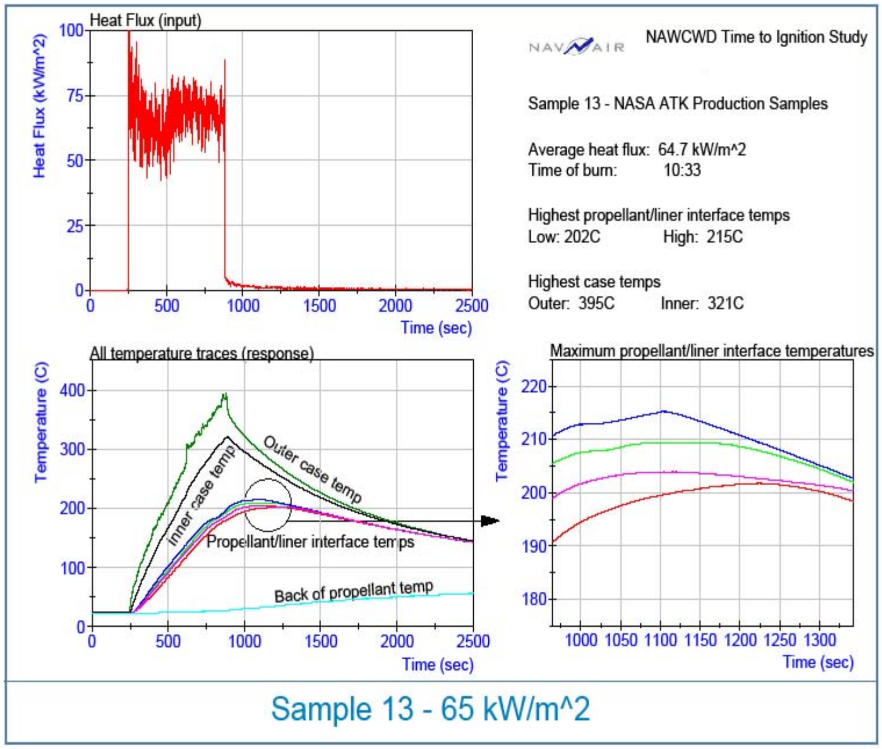


Notes: Flux variability during burn: 42 to 111 kW/$m^2$

FIGURE 16. Sample 13 Data.

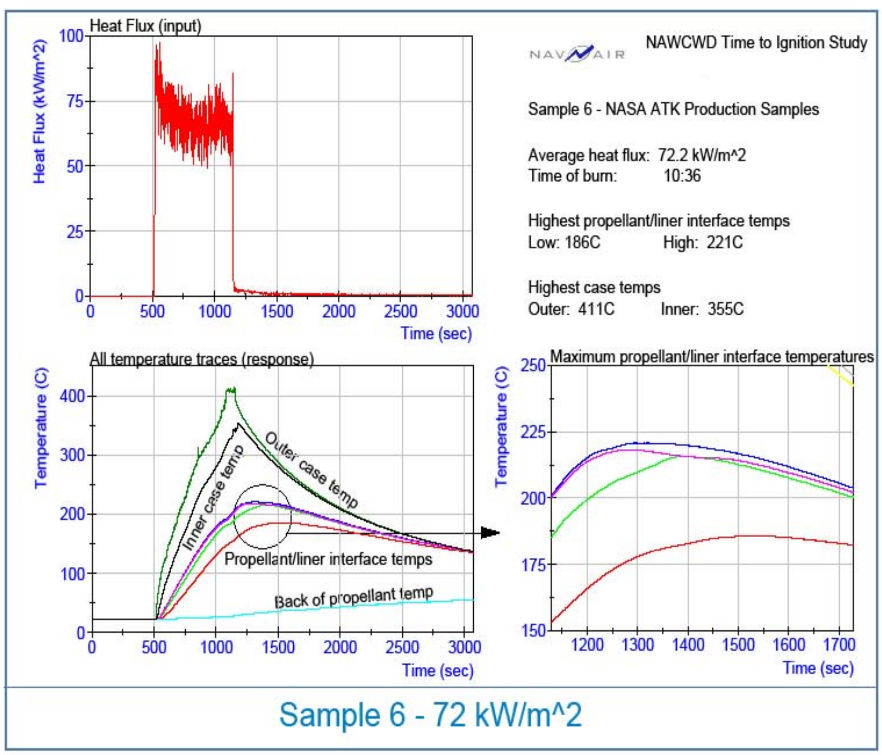


Notes: Flux variability during burn: 49 to 96 kW/$m^2$

FIGURE 17. Sample 6 Data.

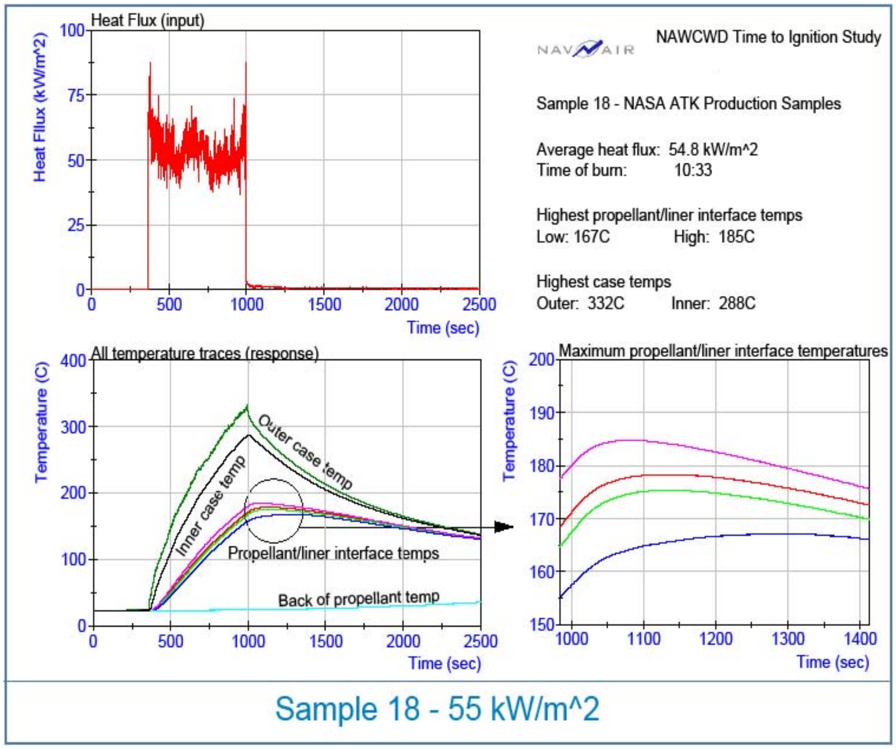


Notes: Flux variability during burn: 37 to 88 kW/m$^2$

FIGURE 18. Sample 18 Data.

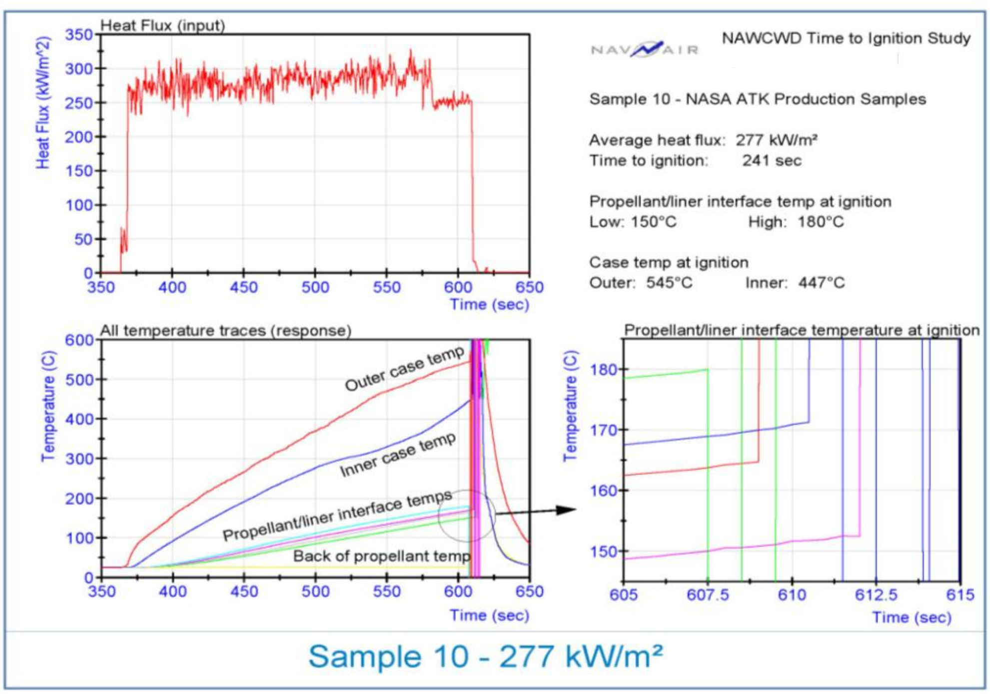


Notes: Flux variability during burn: 230 to 328 kW/m$^2$

FIGURE 19. Sample 10 Data.

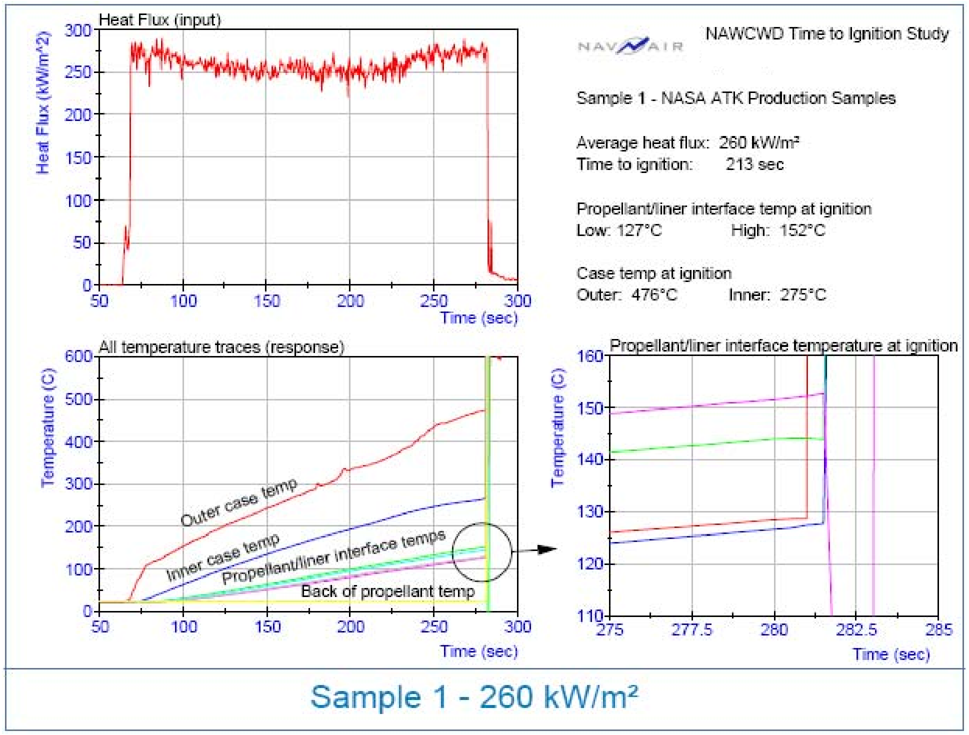


Notes: Flux variability during burn: 221 to 290 kW/m$^2$

FIGURE 20. Sample 1 Data.

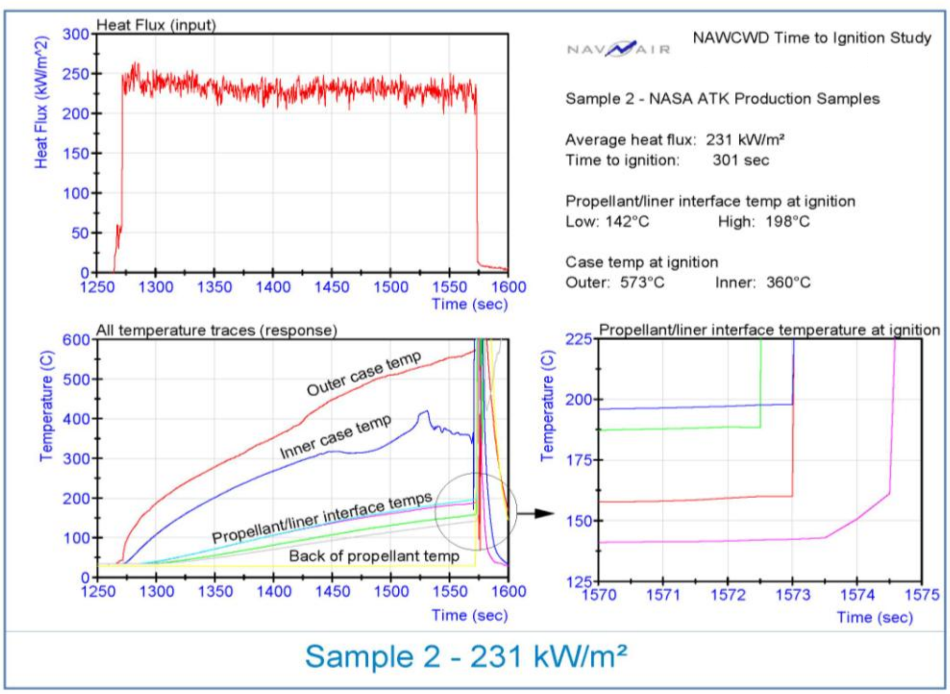


Notes: Flux variability during burn: 200 to 265 kW/m$^2$

FIGURE 21. Sample 2 Data.

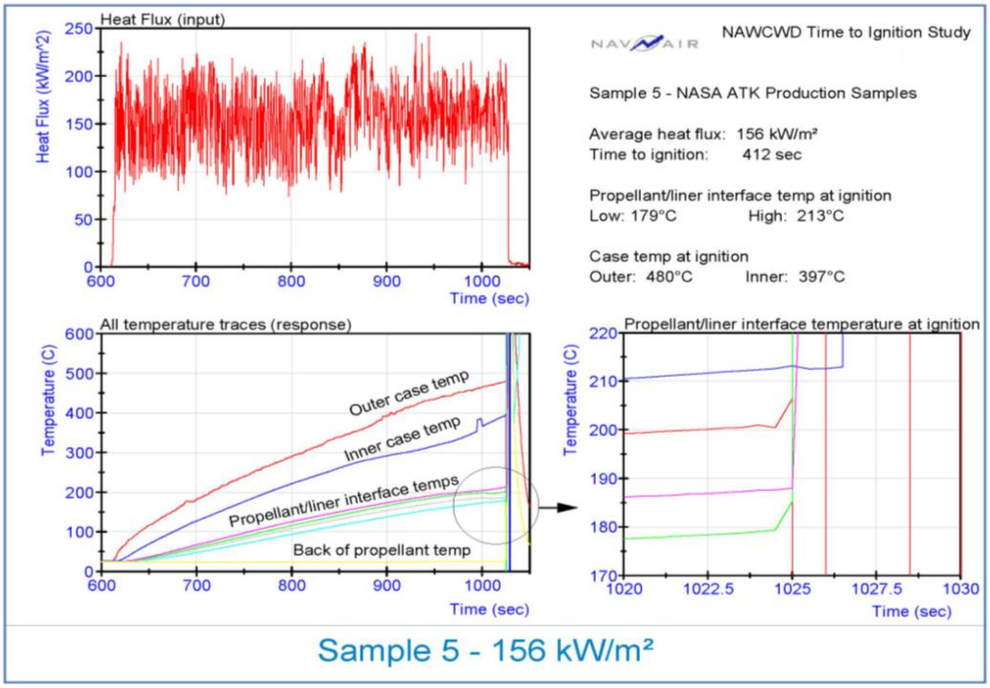


Notes: Flux variability during burn: 74 to 244 kW/m$^2$

FIGURE 22. Sample 5 Data.

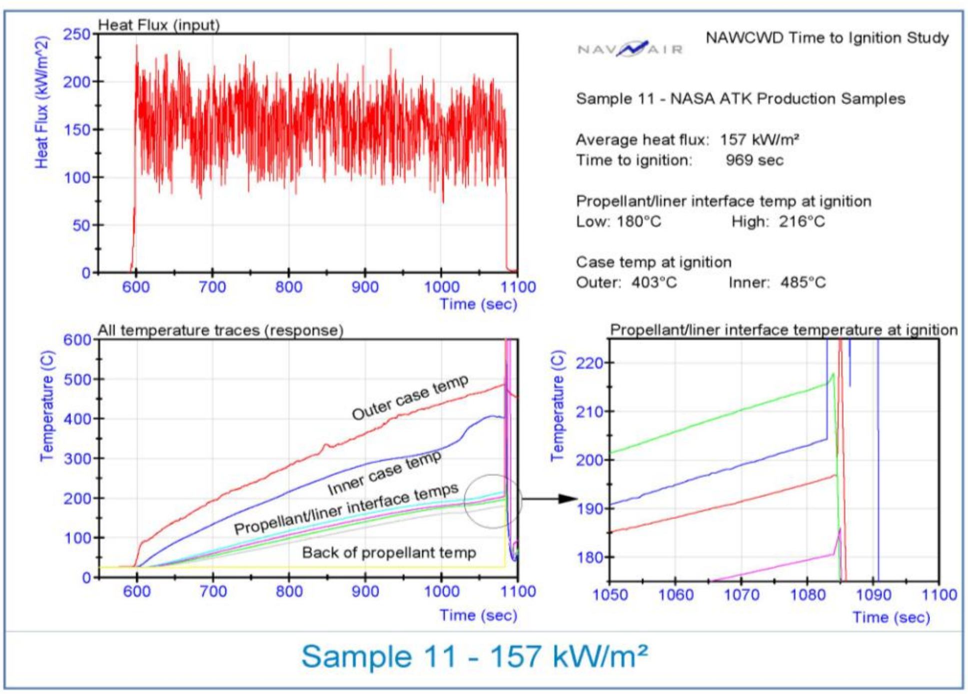


Notes: Flux variability during burn: 73 to 234 kW/m$^2$

FIGURE 23. Sample 11 Data.

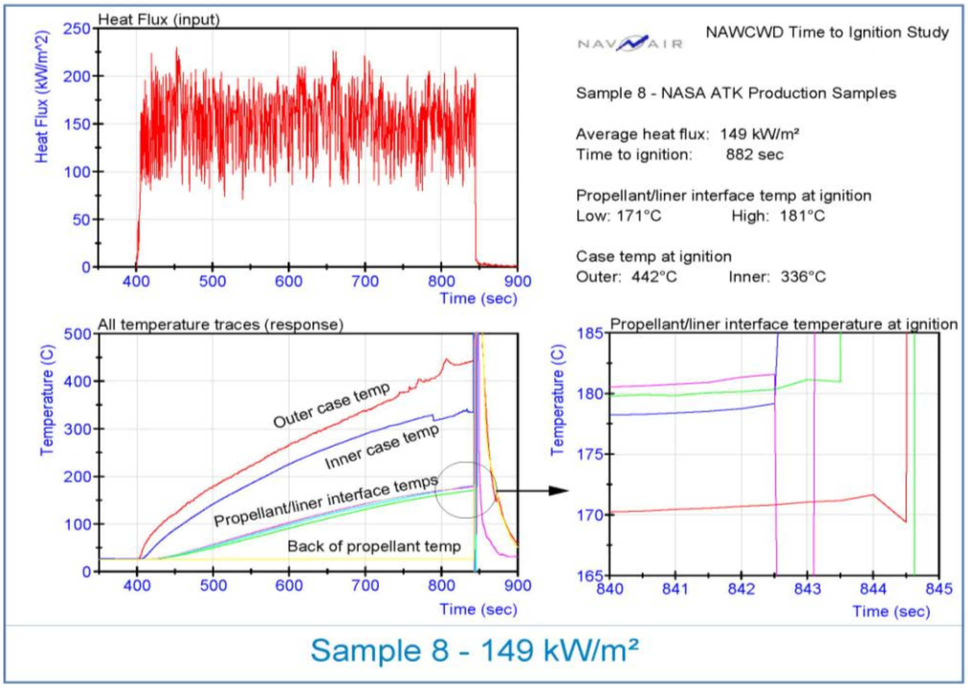


Notes: Flux variability during burn: 71 to 230 kW/m$^2$

FIGURE 24. Sample 8 Data.

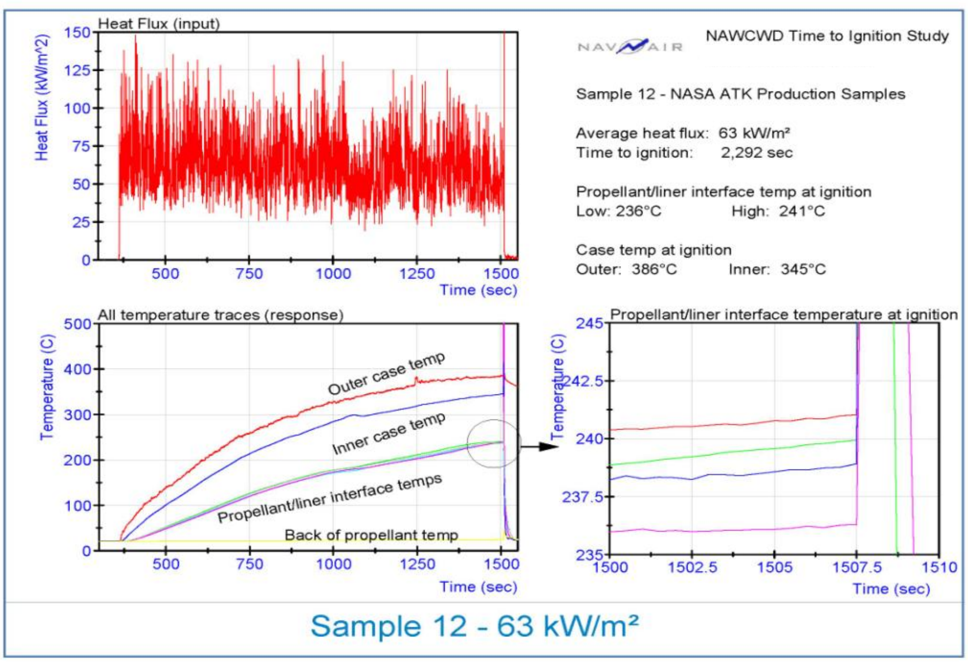


Notes: Flux variability during burn: 19 to 148 kW/m$^2$

FIGURE 25. Sample 12 Data.

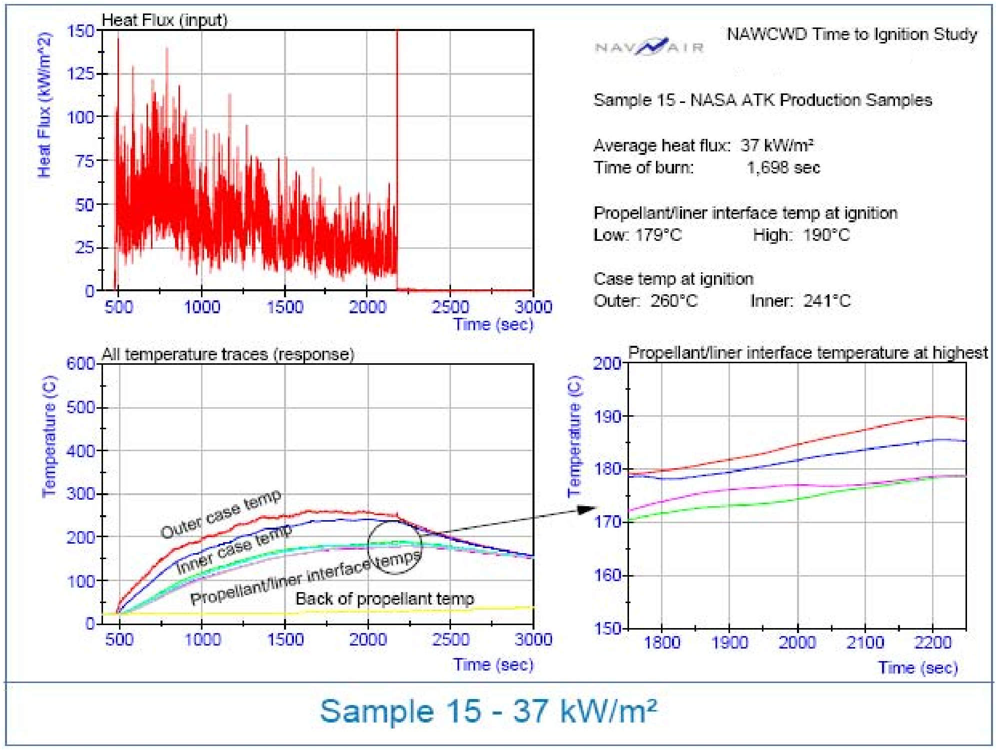


Notes: Flux variability during burn: 6 to 145 kW/m

FIGURE 26. Sample 15 Data.

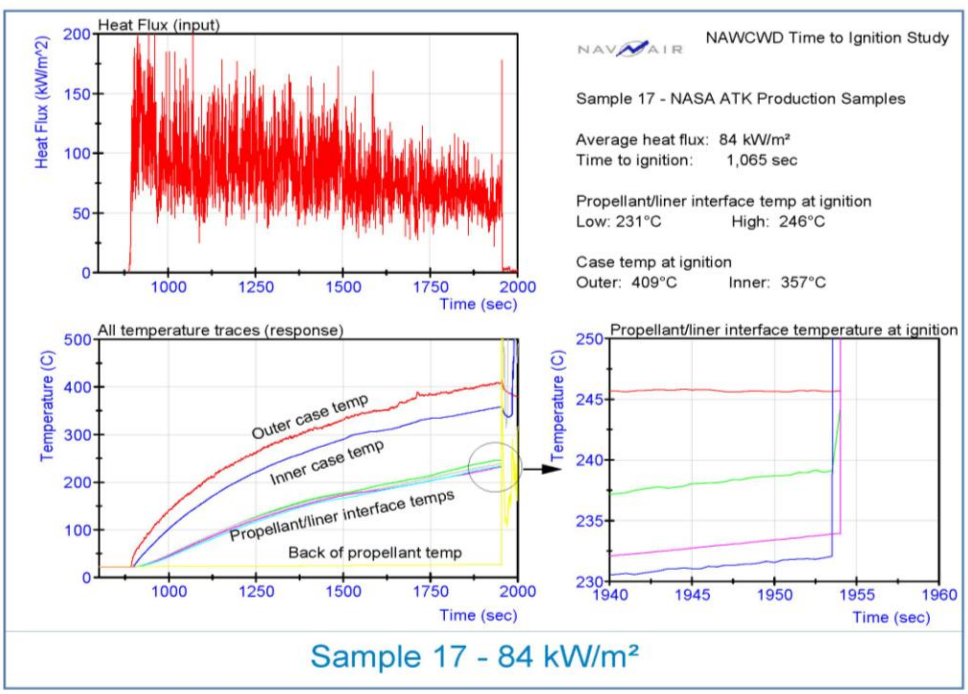


Notes: Flux variability during burn: 22 to 211 kW/m$^2$

FIGURE 27. Sample 17 Data.

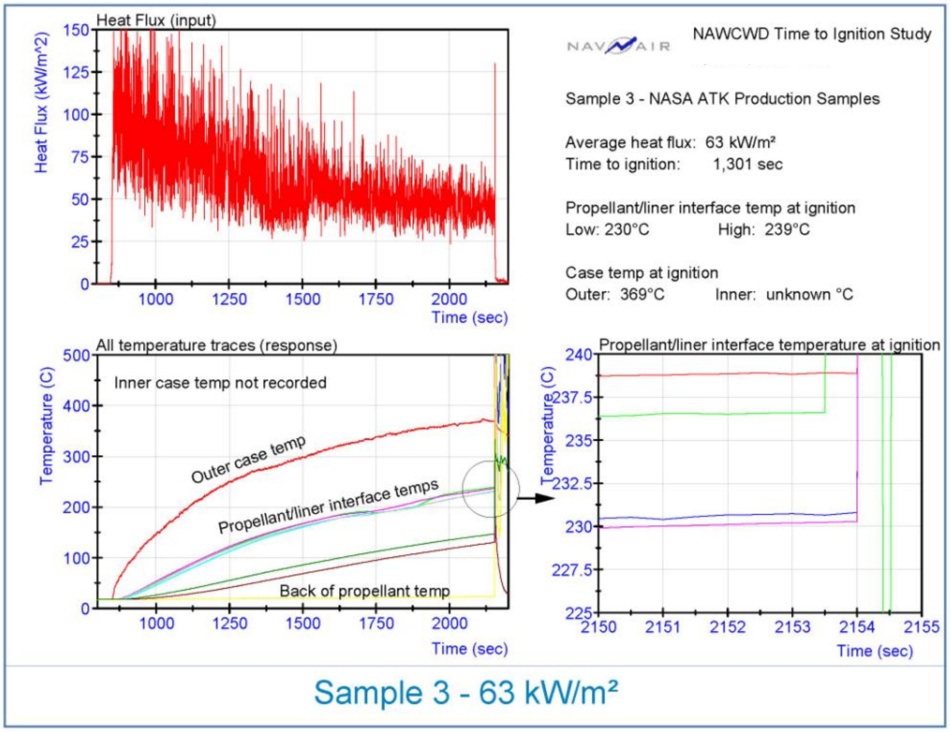


Notes: Flux variability during burn: 24 to 206 kW/m$^2$
No inner case temperature recorded

FIGURE 28. Sample 3 Data.

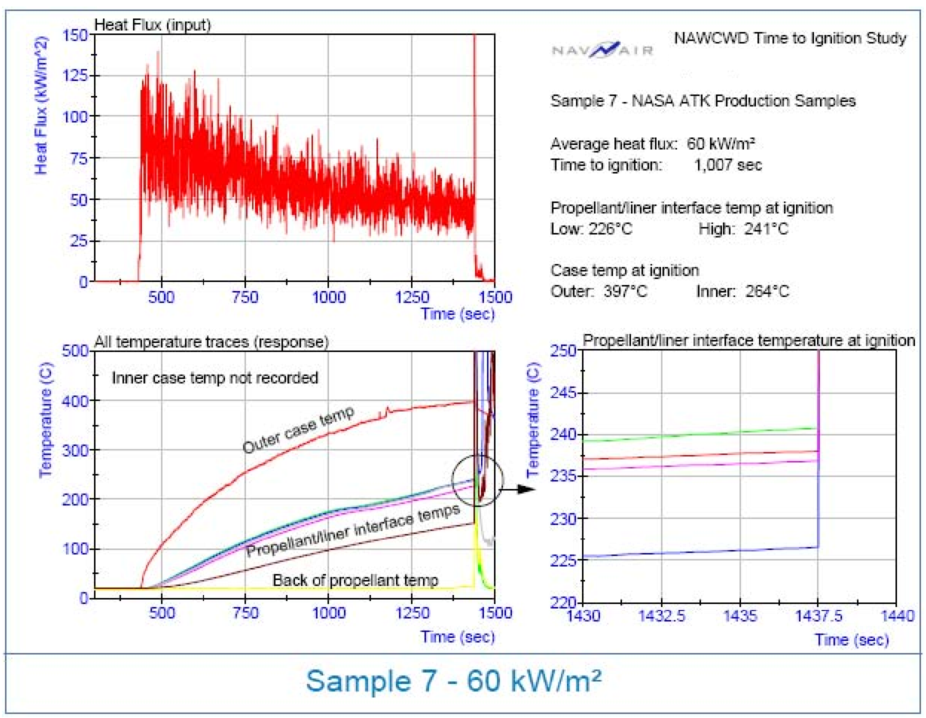


Notes: Flux variability during burn: 24 to 139 kW/m$^2$
No inner case temperature recorded

FIGURE 29. Sample 7 Data.

## DISCUSSION AND CONCLUSION

Expected time to ignition at 300 kW/m$^2$ was 3 to 4 minutes; this ignition time was seen in proof-of-concept samples that had been tested previously, and it was also seen in this test series. At 200 kW/m$^2$, time to ignition was between 4 and 5 minutes. No ignition occurred when samples were heated at 100 kW/m$^2$ for 10.5 minutes (630 seconds). However, when heated for longer times, samples did ignite, except for one at very low flux (37 kW/m$^2$). This represents a validation of the modeling done for the NASA assembly facility. The model predicted that a 300 kW/m$^2$ heat flux applied to the case of the motor would result in a time to ignition of about 4 minutes. The actual data show ignition from 3:01 to 3:40 minutes. The acquired heat flux data was validated by two calibrated heat flux gauges during dry runs and by a single calibrated heat flux gauge during propellant tests.

The torch designed and built for the effort provided a reliable source of heat in the range 50 to 300 kW/m$^2$. A wider range of fluxes (up to approximately 500 kW/m$^2$) is expected with further development. An even more robust torch system will be obtained utilizing the lessons learned from this test series.

The time required for ignition to occur in the bare versus cased samples appears to offer little in the way of correlation between the two data sets. This case is shown in Figure 30.

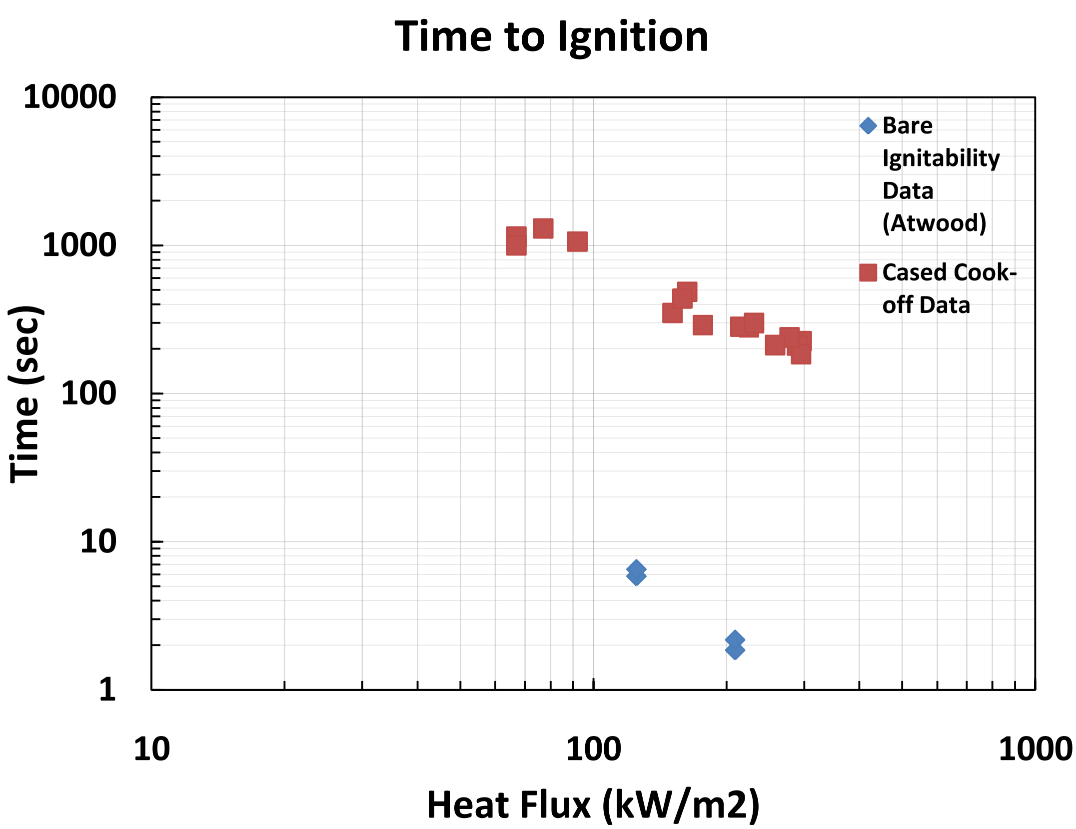


FIGURE 30. Comparison of Bare and Cased Sample Ignition Times Versus Heat Flux.
Data do not include samples 6, 13, 15, 18.

However, analysis reveals that the two sets may actually be closely related. By integrating the heat flux applied to the samples over time, we get a picture of the energy that was driven into the sample by the heat source. The first step in modeling this behavior is to find the average heat flux. This is relatively simple using a spreadsheet, illustrated in Figure 31. Note that higher flux tests show less variability in the flux trace, but lower flux tests show higher variability. This is due to the nature of the flame that provides the heat. Higher flux events require the torch to be closer to the sample, causing the detector to be located in the fairly stable lower regions of the flame. Lower flux events require the sample to be located relatively far from the torch face, where the flame moves around and across the detector to a much greater degree.

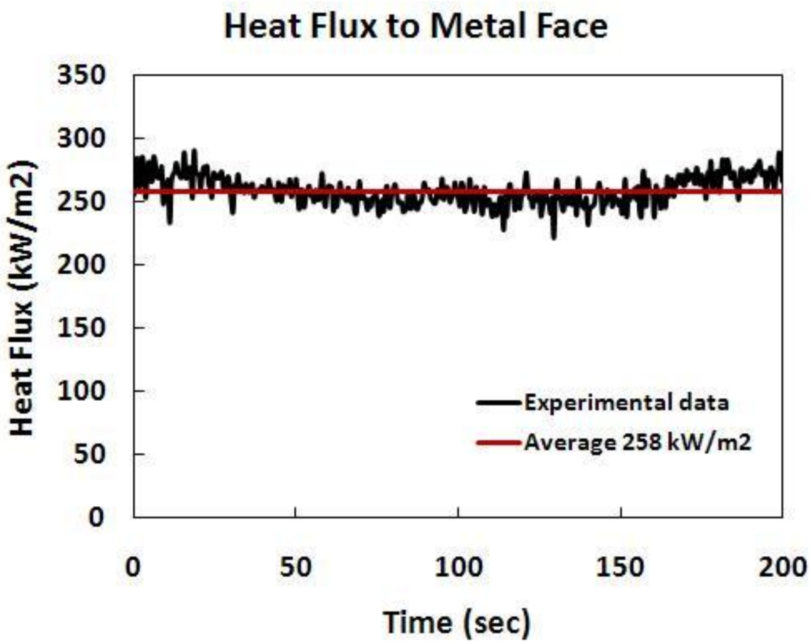


FIGURE 31. Average Heat Flux was Determined. Example is from sample 1.

The next step is to calculate the amount of flux actually reaching the front face of the propellant, at the interface of the liner and propellant. This calculation used the Fluent CFD code with average heat flux, initial temperature, material properties, and boundary conditions assumptions (metal emissivity 0.8, constant heat flux input at front metal face, constant temperature at rear face of propellant, no radial losses, no chemistry or gas formation) as inputs.

The output of this calculation was the heat flux (kW/m$^2$) to the propellant face as a function of time and, by integrating the heat flux over the duration of the test, the total energy flux at the propellant face (kJ/m$^2$). Figure 32 shows an example of the integration of the heat flux over time. The red curve represents the total energy moving past the propellant/liner interface. This example is from the test on sample 1, which ignited at 212 seconds.

The result of time to cookoff is then plotted against total energy flux (Figure 33). The example of sample 1 is plotted with previously acquired data. Sample 1 is the red point and the previous data (bare propellant) points are blue. Note that the axes are switched in this plot (compared to Figure 31), with flux on the bottom (x) axis, and time on the left (y) axis.

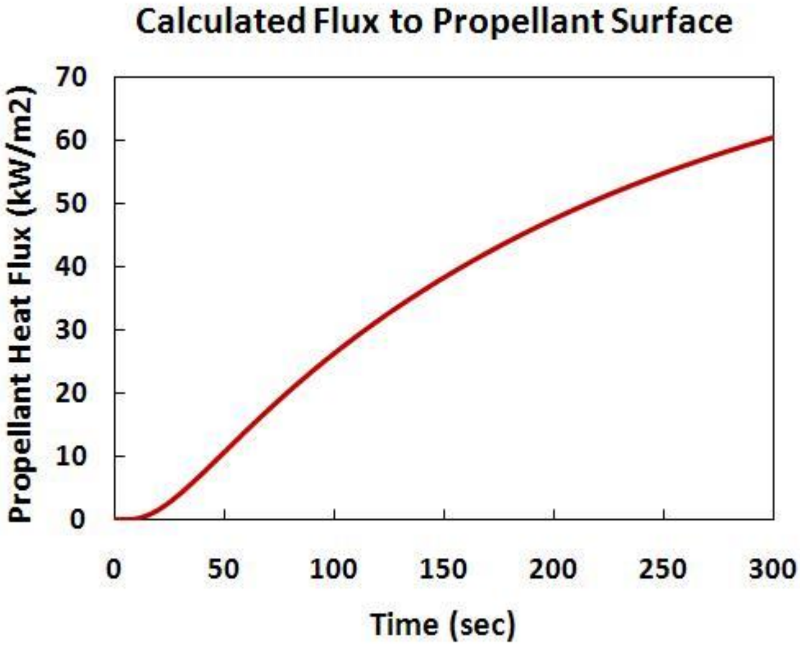


FIGURE 32. Material Properties and Physical Arrangement were Used to Determine the Heat Flux at the Front Face of the Propellant. Heat flux integrated from time zero to ignition. Data from sample 1.

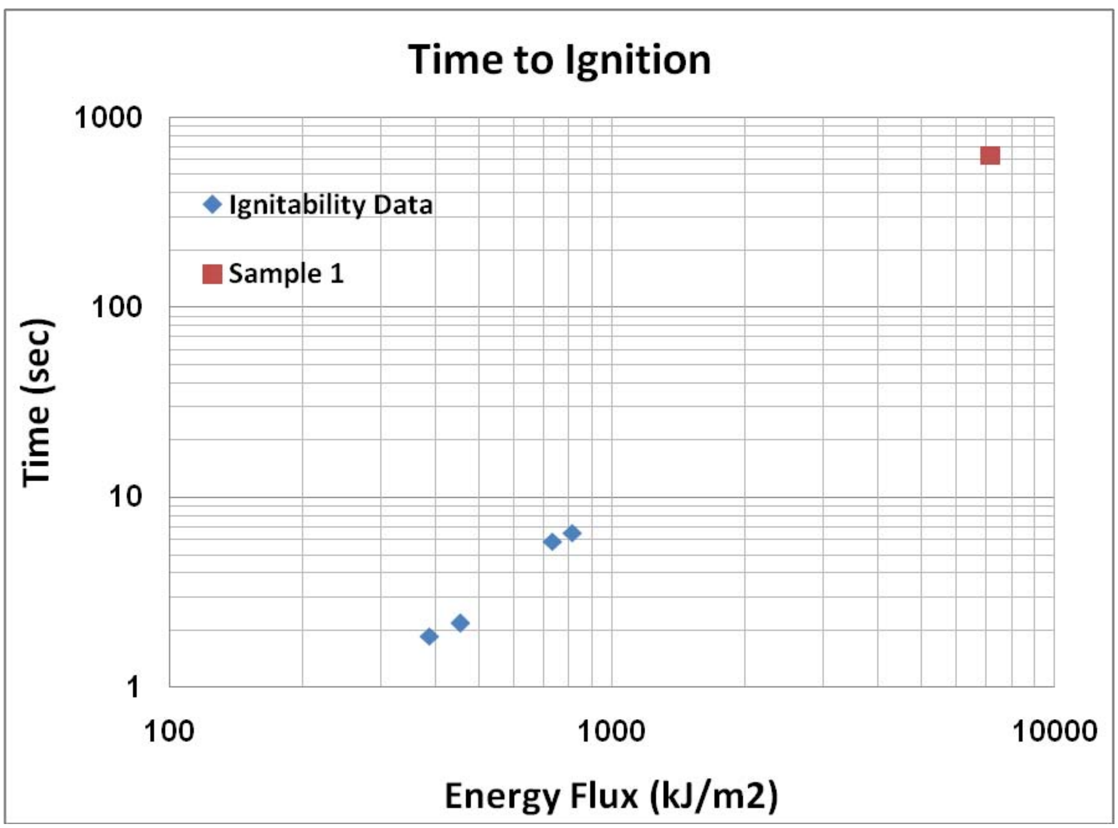


FIGURE 33. Time to Ignition was Plotted as a Function of Energy Flux from Previous Integration. Example from sample 1.

Figure 34 shows the time to ignition as a function of the energy in each sample by unit area. The data from this effort does now correlate to previous ignitability data. Fit to the model's predictive time-to-cookoff line is better at shorter times and less so at longer times. The reasons for this apparent loss of fidelity may be explained in several ways.

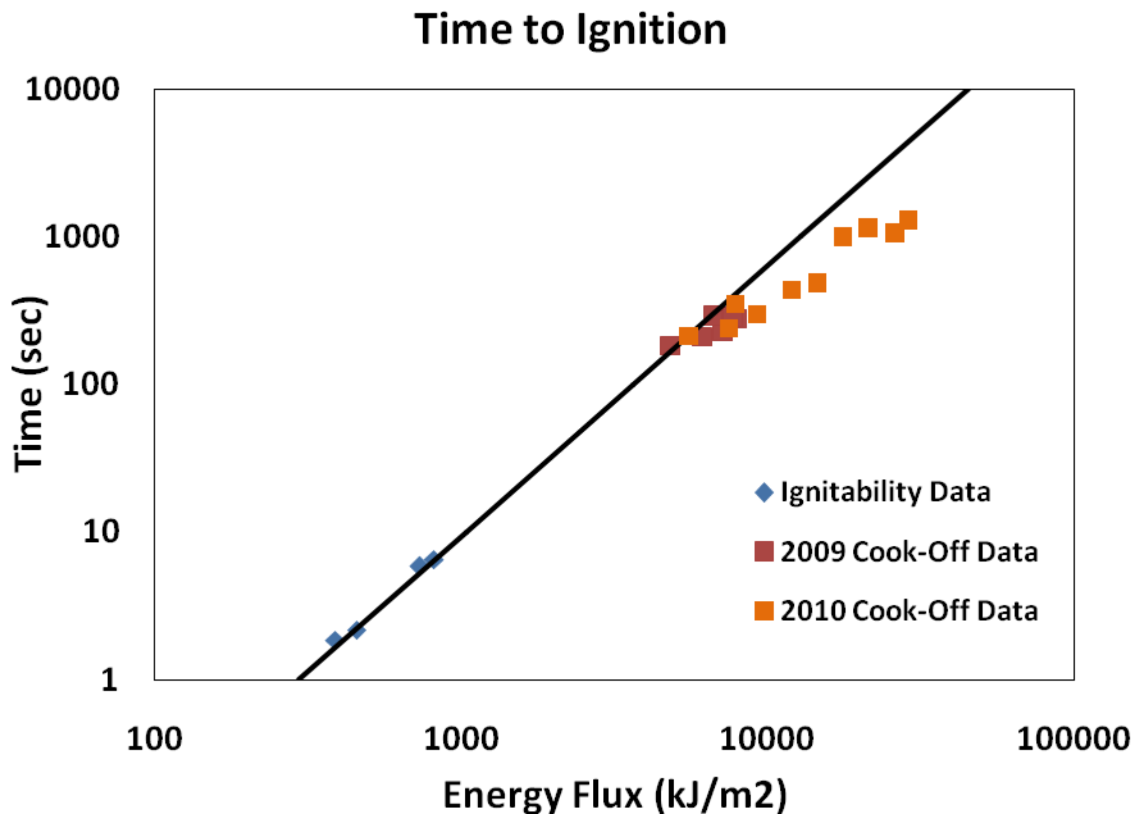


FIGURE 34. Plot of Time to Ignition as a Function of Energy Flux. Bare data is blue. Cased data is red and orange. All 16 cased samples that ignited are included.

The model used to predict system performance makes certain assumptions that are important to consider. First, the model assumes one-dimensional heat transfer and so does not account for radial inputs or any losses. Any heat losses would tend to shift the data to the left. Longer heating times would tend to give rise to increased heat losses. Second, the model does not account for any changes in contact resistance, so any voids that are generated by pyrolysis or other decomposition of the materials in the sample are not taken into account. If void generation does in fact occur, it would shift the results to the right and away from the model's prediction. A model that accounted for surface contact discontinuity changes would bring the actual results more into line with the prediction. Finally, material properties are very important to the model and have great effect on the results. Properties are needed at high temperatures, and the properties may even be heating-rate dependant. So use, here, of rudimentary material properties, some of which assume static conditions, may limit the accuracy of the results.

One of the interesting results from this model is the predictive ability it may offer. Figure 35 shows how heat fluxes may be superimposed on the energy flux/time plot to indicate predicted time to cookoff. Clearly, the ability to predict time to cookoff from a flux input, regardless of whether the energetic material is bare or cased, from a single model could be of enormous value. Further refinement of the model will aid such development. Obviously, different propellant systems use different physical arrangements and different materials, but for a single system, this ability to predict cookoff offers great benefits to systems safety analysis. Adapting the model to other systems should be relatively simple.

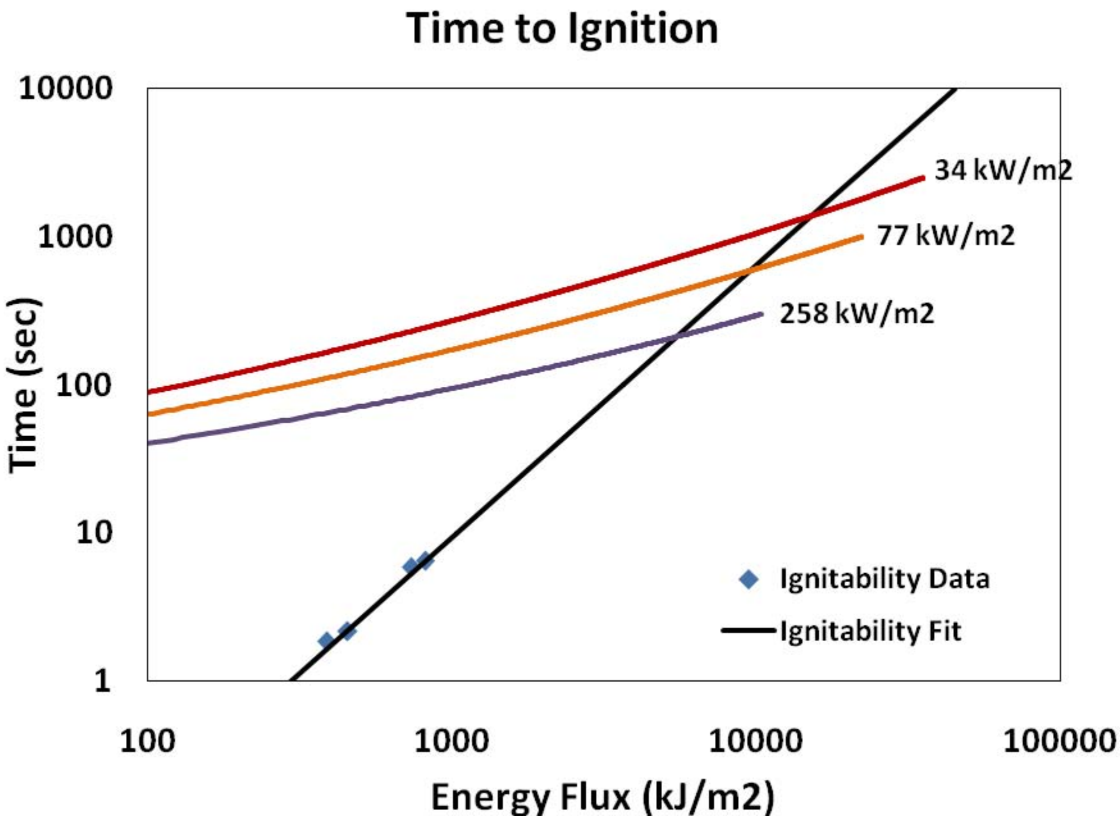


FIGURE 35. Plot of Time to Ignition as a Function of Energy Flux, with Heat Flux Inputs Inserted to Provide Cookoff Time Estimation.

Ignition was expected to occur at the propellant/liner interface, since the propellant at this interface was the closest to the heat source and therefore expected to be the hottest. Bare propellant ignition testing has shown that similar propellant formulations ignite when the surface temperature reaches 260 to 308°C (References 1 and 2). However, the actual temperature of the propellant/liner interface, at ignition, is difficult to measure accurately. Several independent experiments have obtained temperature results, under similar conditions, that seem low (References 3and 4). It is believed that a poorly understood interaction between the thermocouple bead and the propellant grain and liner in an environment with a large thermal gradient leads to a lower-than-expected thermocouple temperature. However, no adequate explanation was available at the time of publication.

An investigation is underway to discover the cause of this phenomenon, since several previous tests have seen the same effect. To explore the conditions of high thermal gradient temperature sensing in a polymeric matrix using thermocouples, we recommend a simple series of experiments to determine actual thermocouple performance in a similar environment. Embedding various-sized thermocouples in a matrix of high-density polyethylene or similar polymer, whose properties are well-characterized, and heating it to determine the role of bead size and thermal gradient would provide insight into the temperature phenomenon seen in this test series. Additionally, a method for ensuring thermocouples remain at the liner/propellant interface during casting without the use of epoxy is being developed.

In conclusion, the cookoff of 16 samples (and 4 no-go samples) described in this report resulted in expected times to ignition, but ignition occurred at lower-than-expected temperatures at the propellant/liner interface. This test series shows ignition through the case of other motors in the facility is not likely due to the time required for ignition to occur. The 130 second burn-time of a candidate SRBreplacement rocket that underwent inadvertent ignition in the KSC VAB is too short to achieve ignition through the case of other motors in the facility. According to the results of this test series, the inadvertently ignited motors would have to burn for at least an additional 50 seconds to cause ignition in other motors through the case.

## REFERENCES


1. T. P. Parr and D. M. Hansen-Parr. "Thermal Properties Measurements of Solid Rocket Propellant Oxidizers and Binder Materials as a Function of Temperature," 34th JANNAF Combustion Subcommittee Meeting Proceedings, October 1997.

2. G. Lengellé, A. Bizot, J. Duterque, and J. Amiot. "Ignition of Solid Propellants," *Rech. Aerosp.*, Vol. 2, pp. 1-20, 1991.

3. J. E. Cocchiaro. "Subscale Fast Cookoff Testing and Modeling for the Hazard Assessment of Large Rocket Motors," Chemical Propulsion Information Agency CPTR-72, March 2001.

4. K. P. Ford et al. "Subscale External Fire/Fast Cookoff Testing Results," 2008 DDESB Seminar Proceedings, August 2009.

# Ignition Results of Sub-scale Hazard Division 1.3 Propellant Samples


NAWCWD Code 474200D

Fire Science & Technology Office
China Lake, CA

E. Wilson, E. Washburn, M. Gross, E. Sievert,
D. Wooldridge, J. Daly,
S. Barry, S. Stover, T. Laker, J. Covino


July 14, 2010

# Background

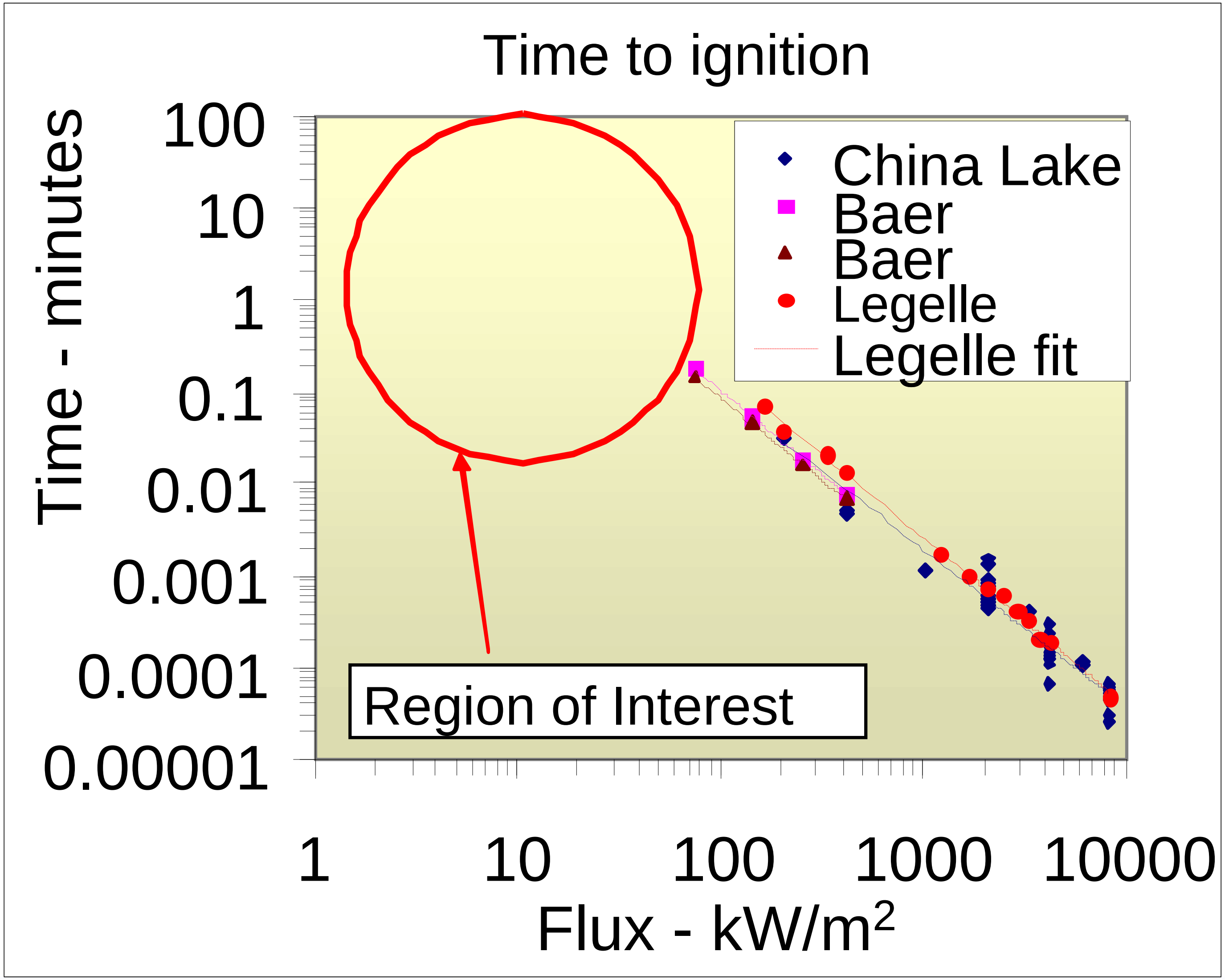

Time to ignition
Time - minutes
100
10
1
0.1
0.01
0.001
0.0001
0.00001
China Lake
Baer
Baer
Legelle
Legelle fit
Region of Interest
1
10
100
1000
10000
Flux - kW/m2

# Sample Design

# Thermocouple Locations – Side View

- Full-scale analog
- Incorporated seven thermocouples
    - One on outside of case
    - One on inside of case
    - Four at propellant/liner interface
    - One at the back

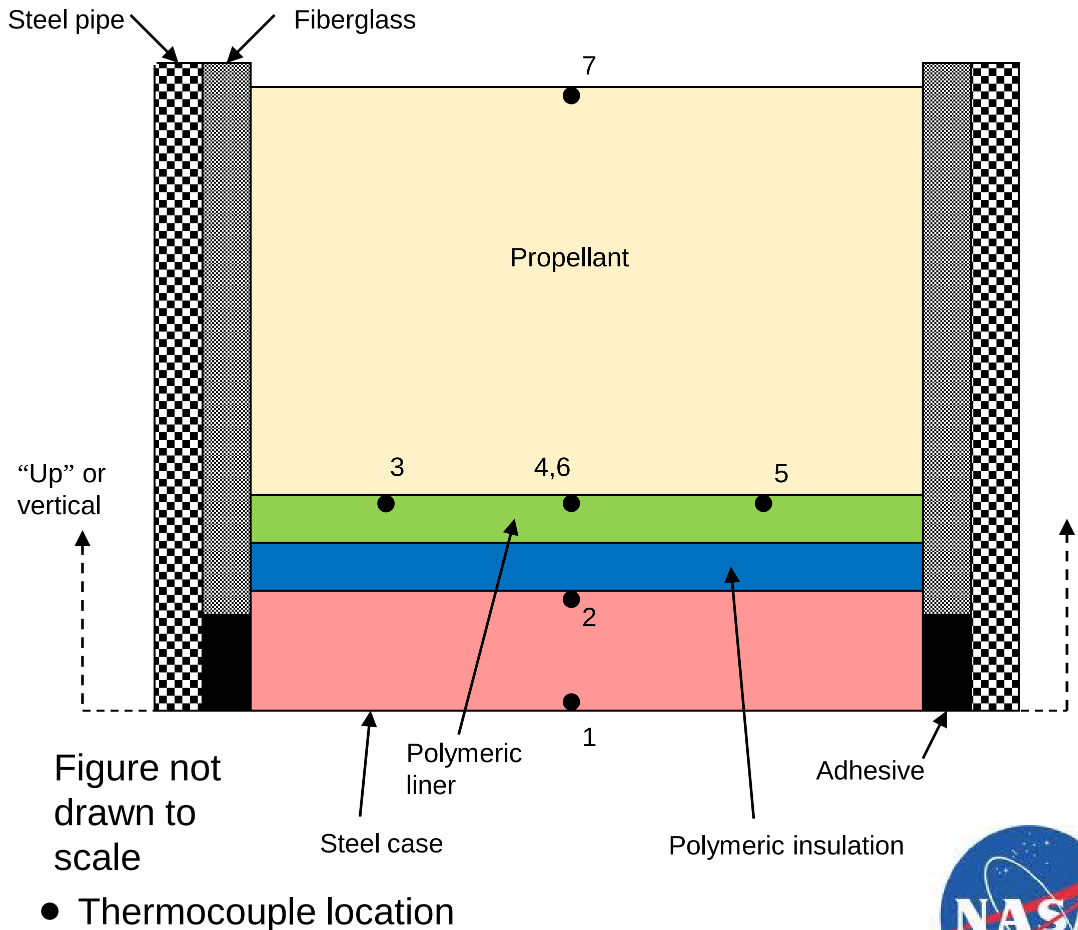

# Thermocouple Locations – Top View

- ½" (1.3 cm) D6AC steel
- Annulus filled with adhesive
- Case, insulator, liner, & propellant comprised the sample

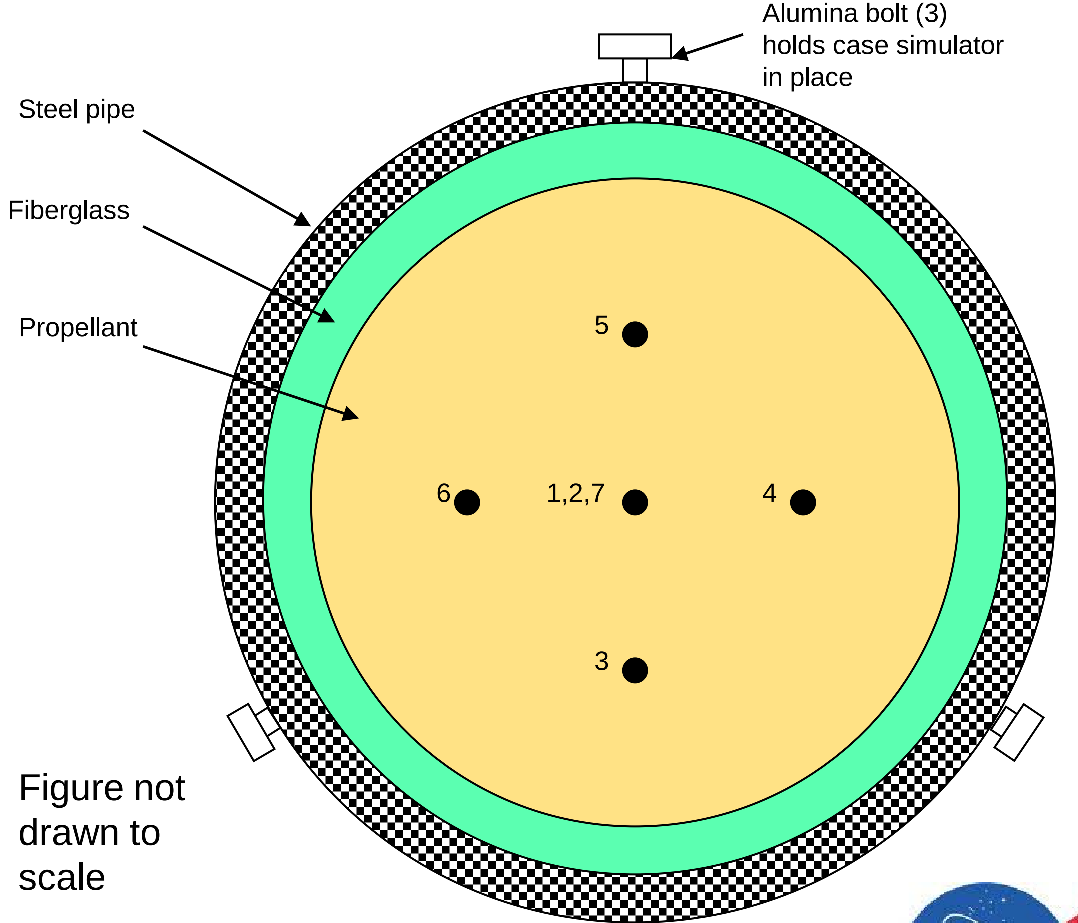


Figure not drawn to scale

● Thermocouple location

# Test Design

- Flame cannot reach annulus nor cause radial heating
- Gardon gauge sensor
- Validation done with another gauge at sample location

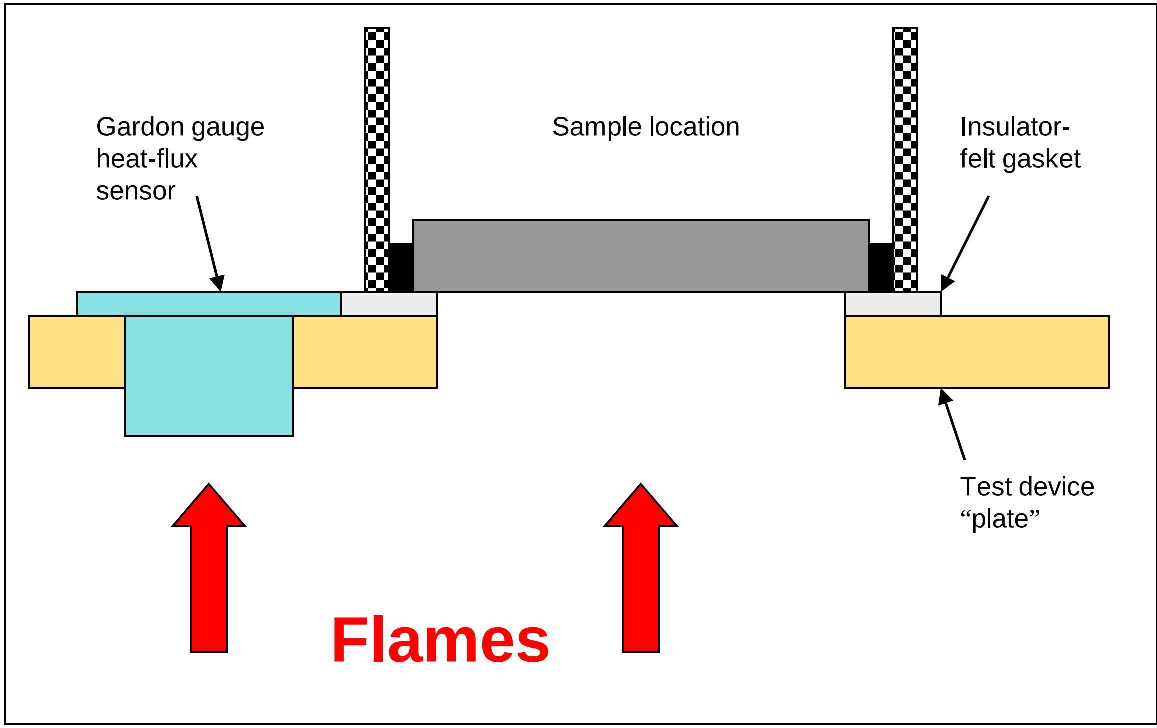

# Torch

- Flame in 2-parts - bright fingers and residual plasma
- Heat flux varied by changing the distance to the sample
- Result is vastly different from laser
- 450 – 500 kW/m² flux possible w/ tweaks

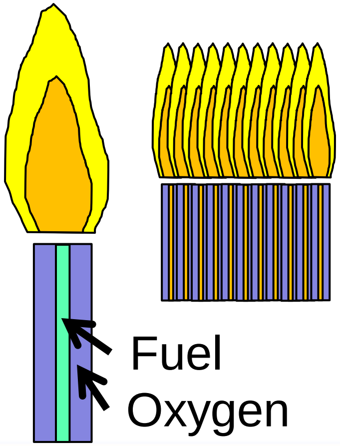


# Test Procedure

- Samples heated with selected level of heat flux until ignition occurred
- Acquired heat flux, temperature, and time to ignition

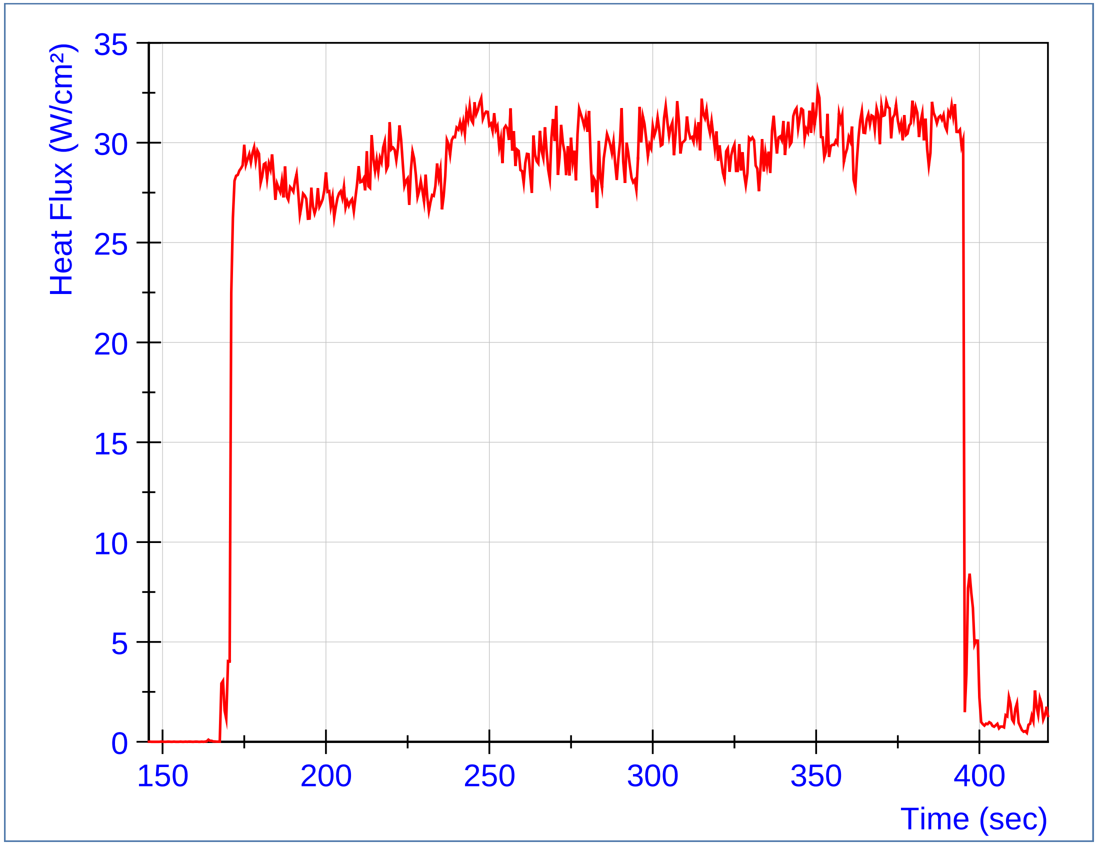

# Time to Ignition

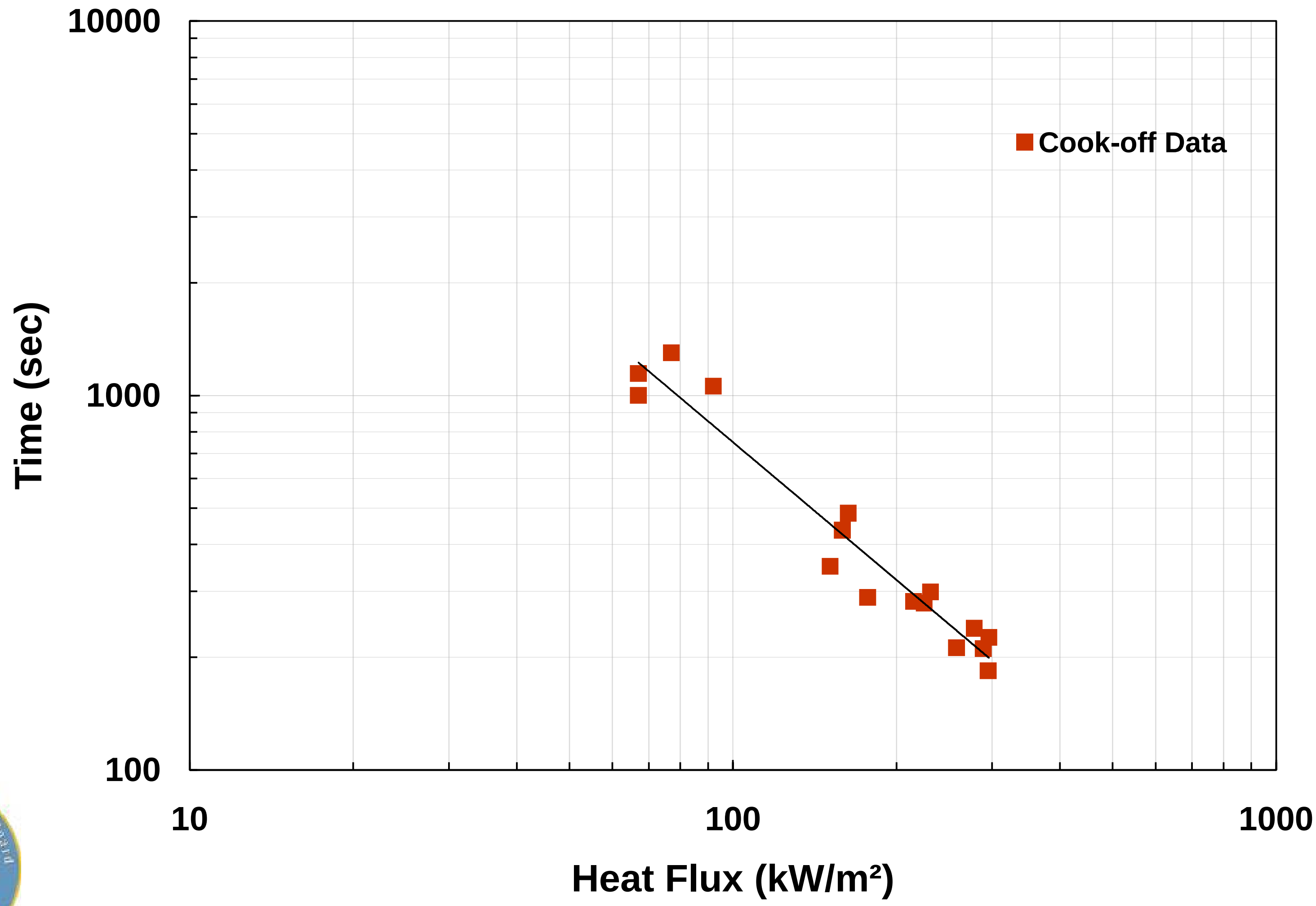

# Comparison

## Time to Ignition

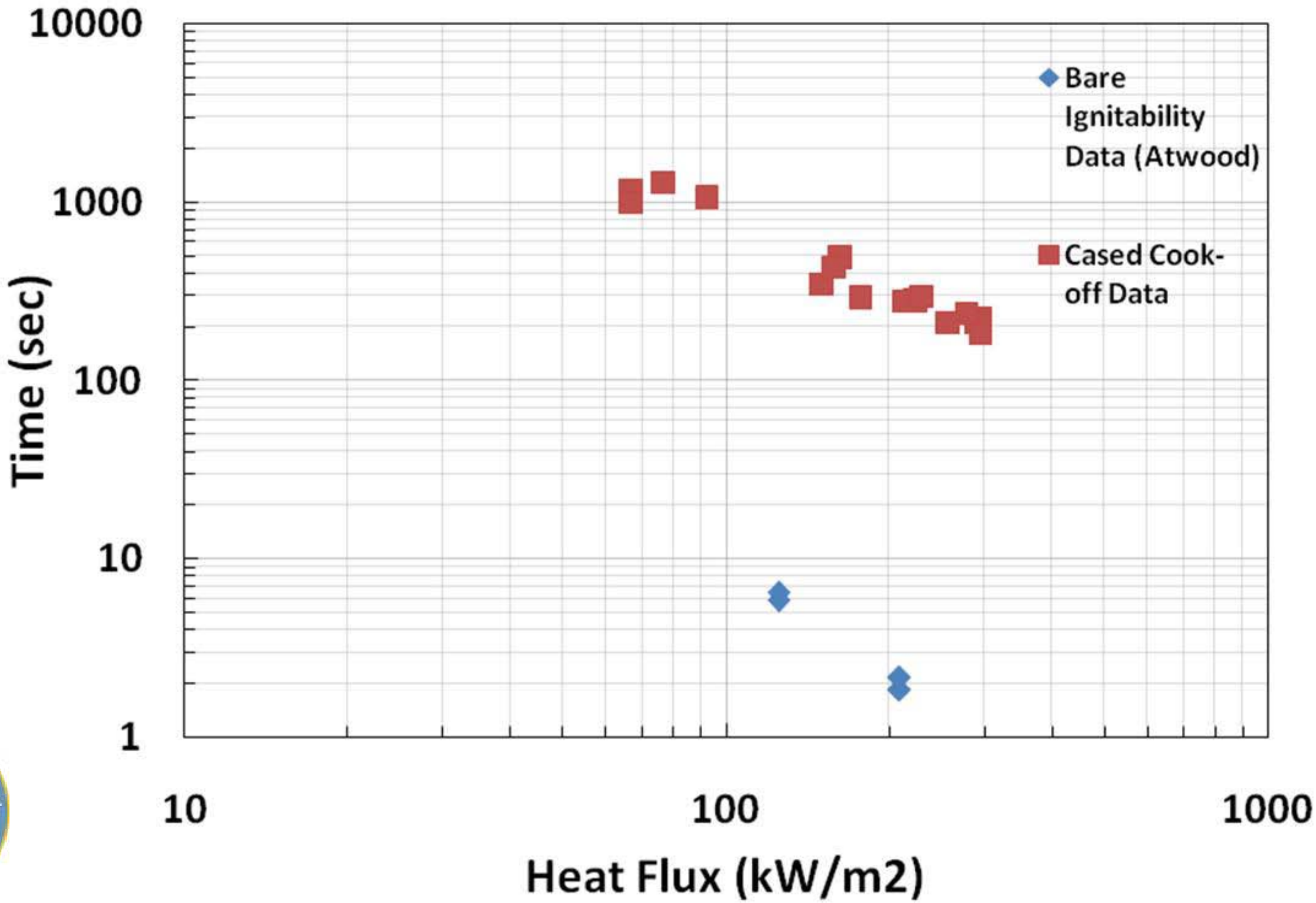

# Assumptions

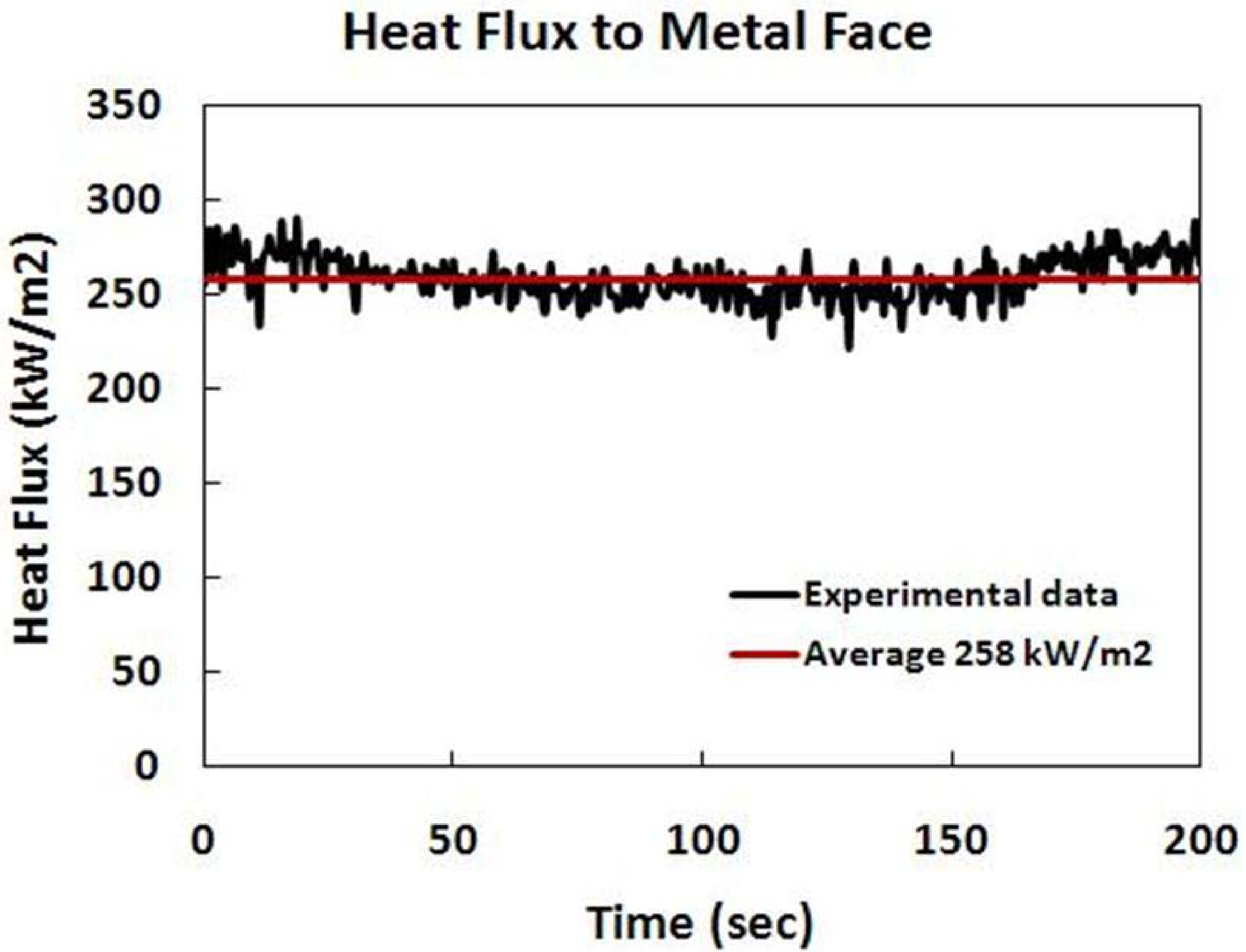

# Integration

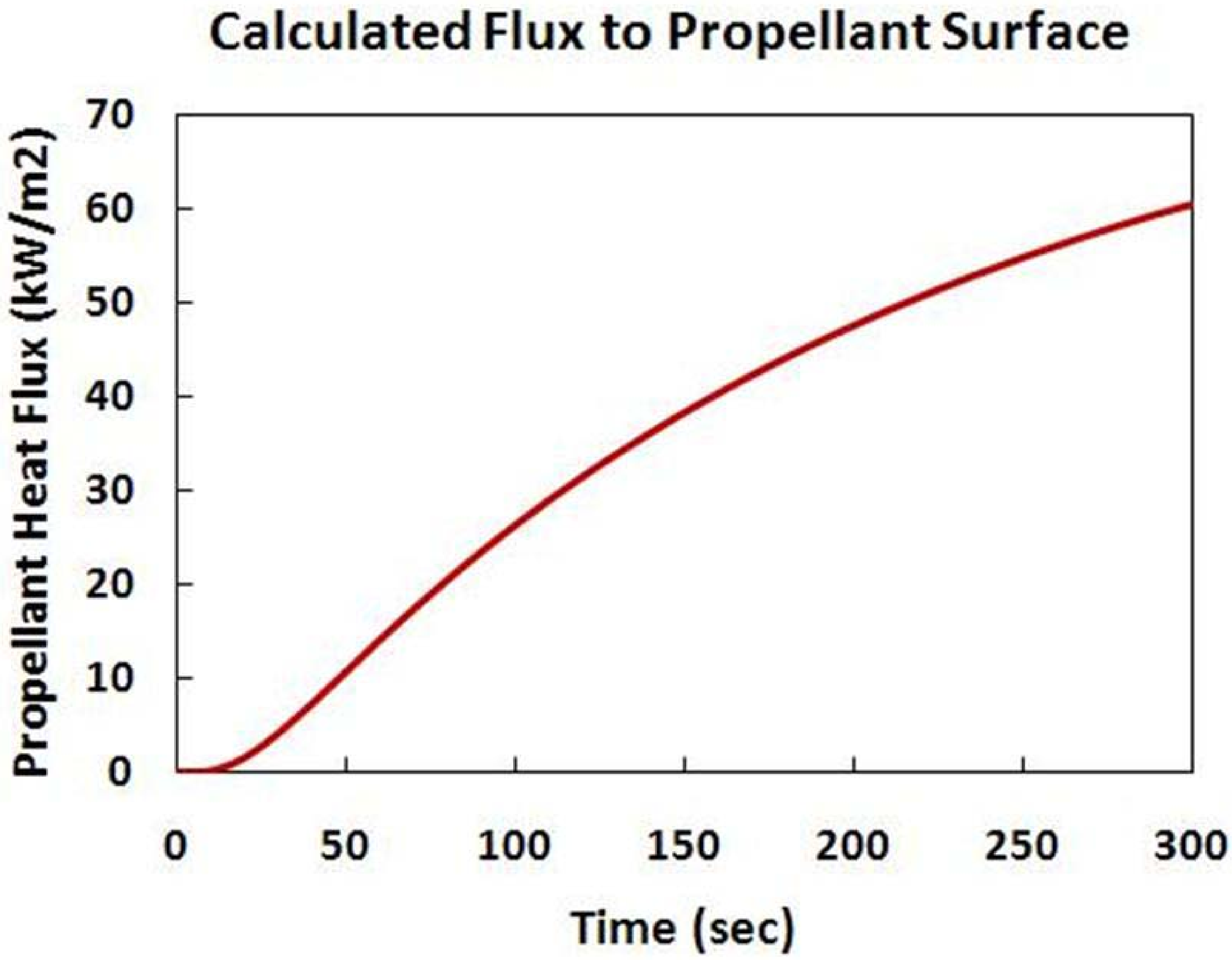

# Interpretation

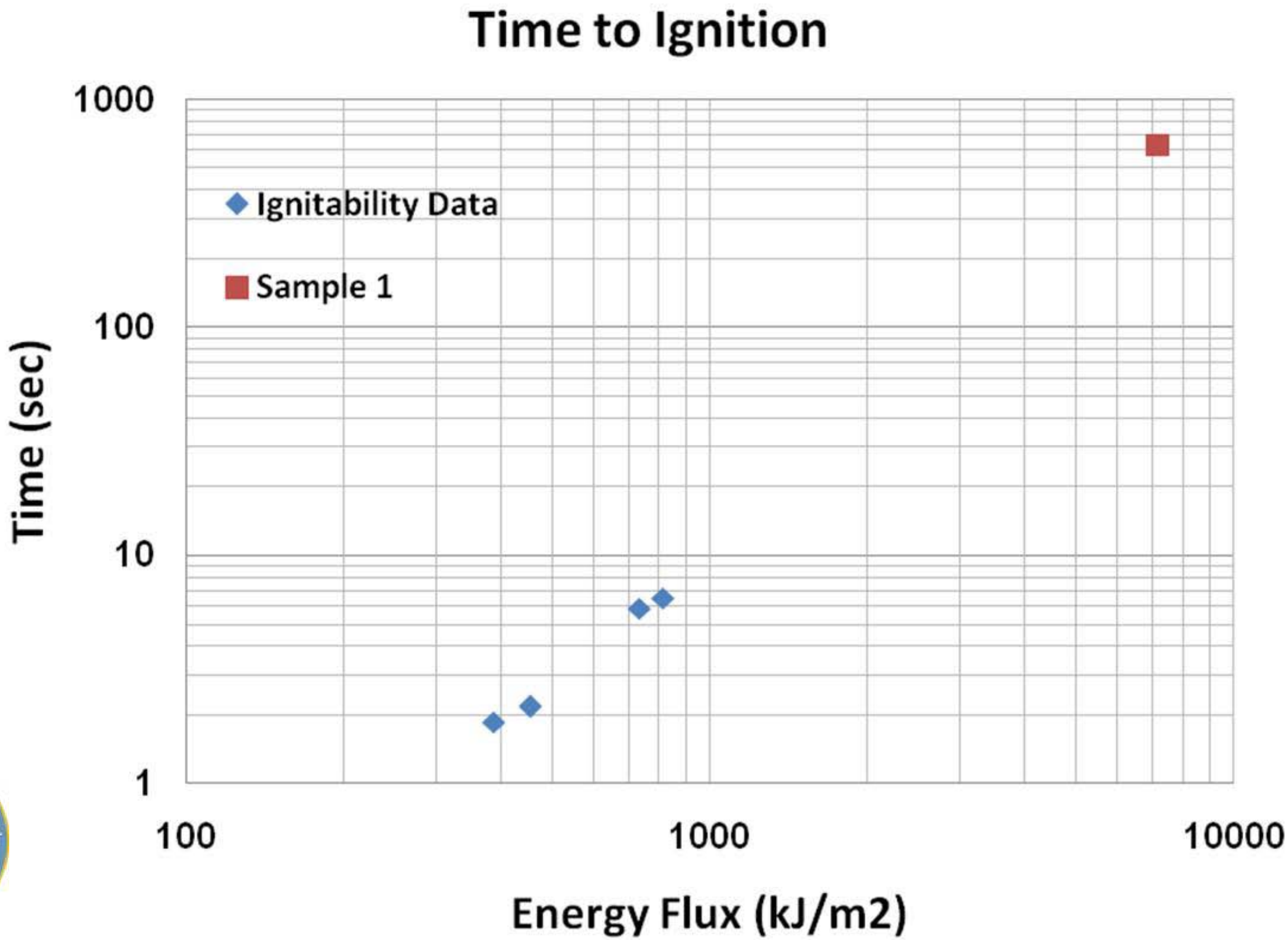

# Interpretation

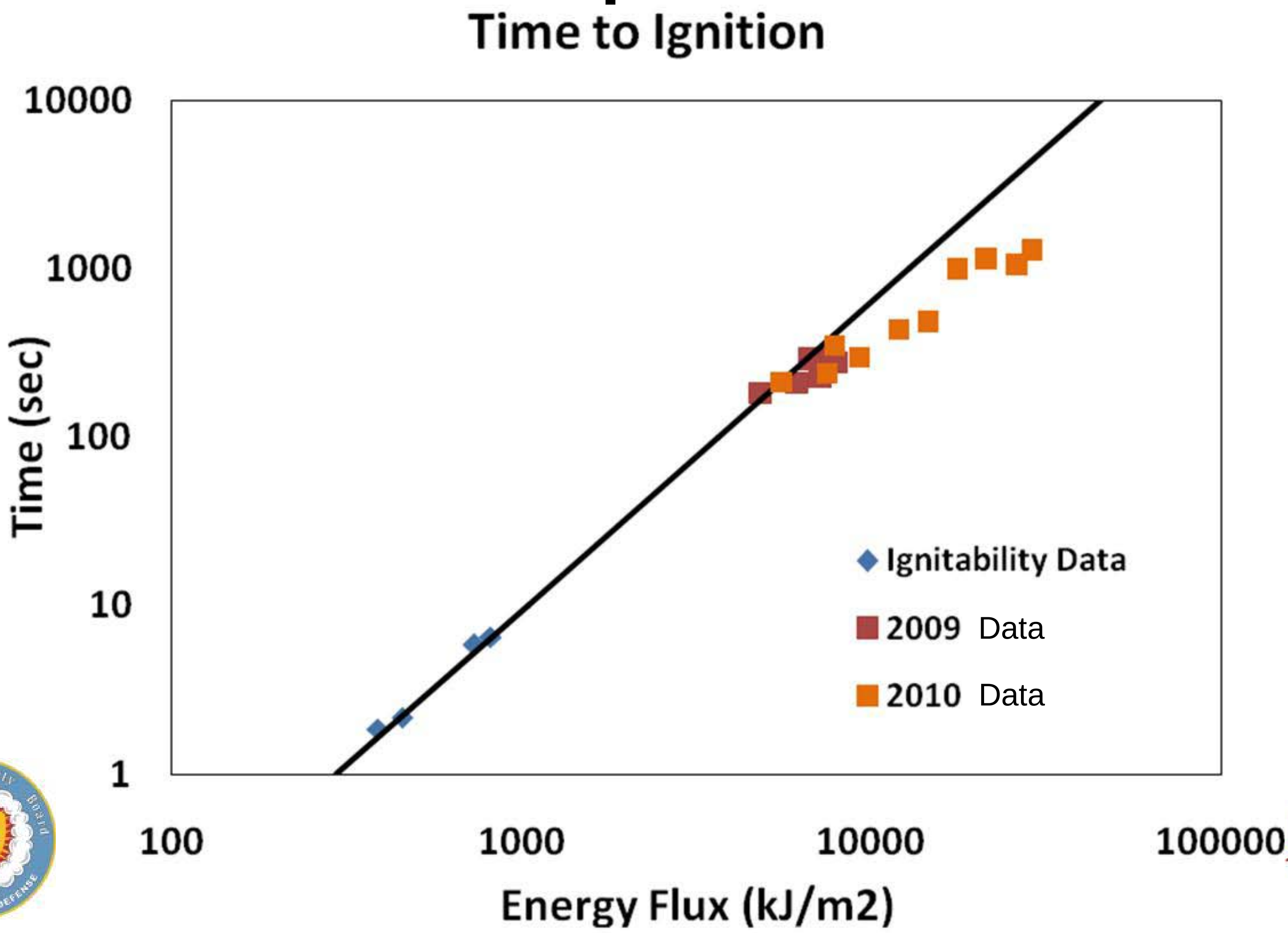

# Interpretation

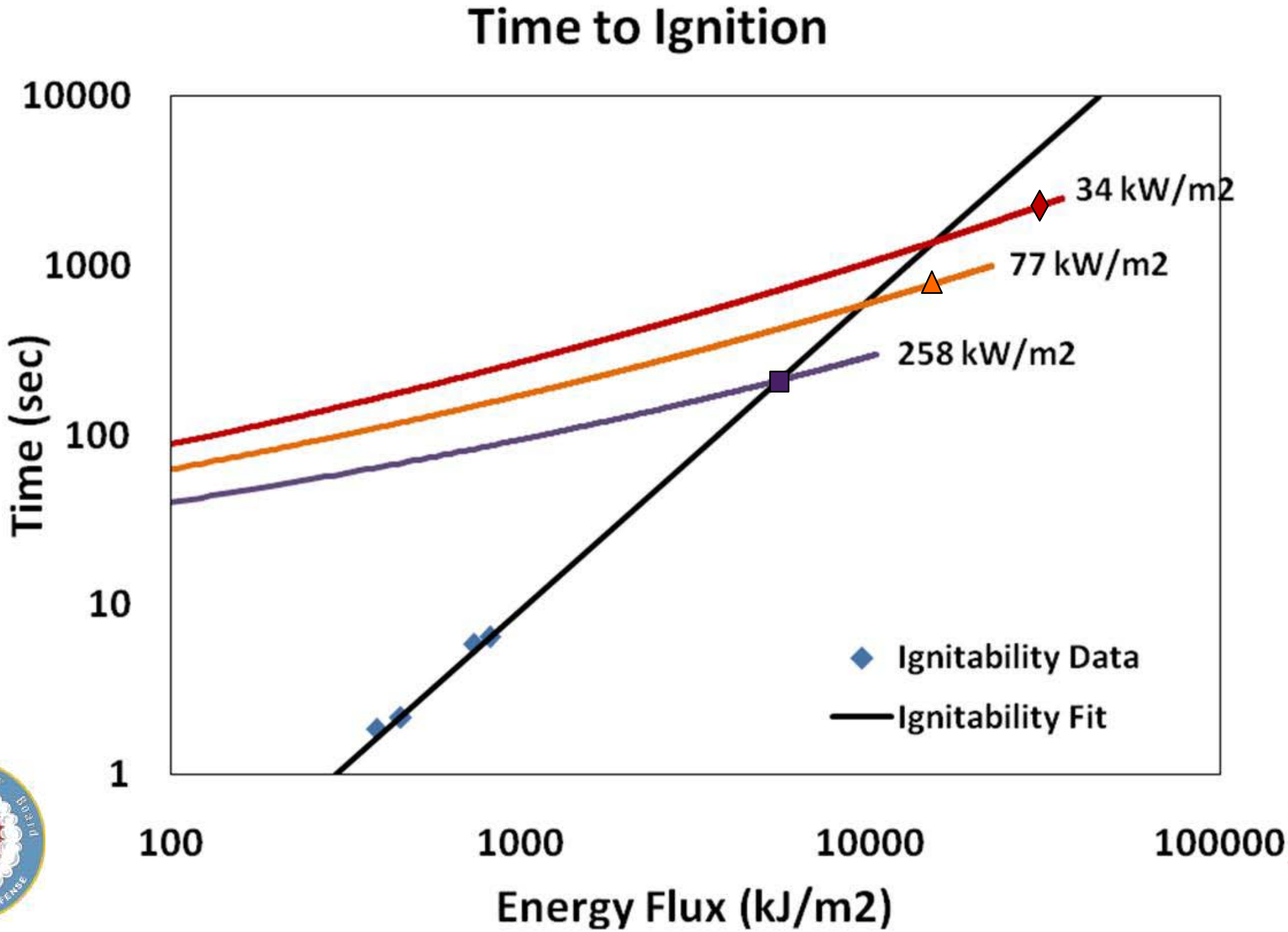

# Summary

- 20 samples tested, 16 ignited
- Lower than expected temperature at propellant/liner interface at ignition – especially for higher flux tests
- Time to ignition as expected – approximately three to four minutes at 300 $kW/m^2$
- Low-flux data acquired (60 $kW/m^2$)
- Post-processing of data shows interesting observation

# Future Work

- Improve torch and sample holder device
- Bomb coating
- HD 1.1 material
- Better temperature data for liners, insulators, propellants

# Questions?

# Backup Slides

# Fire Science & Technology Office (FSTO)

- Fleet/Force firefighters are main customers
- Insensitive Munitions (bomb coating) work done at China Lake
- Develop fire/combustion solutions for fleet/force needs on laboratory, intermediate, and full scale
  - Lab scale: Fire dynamics lab & Fire Chemistry Lab
  - Intermediate scale: Burn room test facility
  - Full scale: Flight Deck Fire Test Facility
- Evaluate shipboard and land-based firefighting tactics, equipment, and agents.  Make doctrinal and acquisition recommendations
- Work with Weapons Survivability Laboratory (on-center) to provide fire and thermal event research and testing for vehicles and aircraft